

# Advances in the use of carbonaceous scaffolds for constructing stable composite Li metal anodes

CHEN Yue<sup>†</sup>, ZHAO Lu-kang<sup>†</sup>, ZHOU Jun-long, BIAN Yu-hua, GAO Xuan-wen\*,  
CHEN Hong, LIU Zhao-meng, LUO Wen-bin\*

(School of Metallurgy, Northeastern University, Shenyang 110819, China)

**Abstract:** Compositing lithium metal anodes (LMAs) with carbon-based materials has been given much attention because of the latter's low density, high mechanical strength, stable electrochemical properties, and large specific surface area. Such a composite LMA stands out because of its ability to reduce the volume expansion, lower the local current density, and provide active nucleation sites for uniform Li<sup>+</sup> plating. Recent research advances in carbon-based materials as scaffolds to make composite anodes are reviewed, including composites with pure metals and their alloys, and compositing strategies to improve anode stability.

**Key words:** Lithium-metal batteries; Carbon-based materials; Carbonaceous-based scaffolds; Preparation techniques; Dendrite growth

## 1 Introduction

At present, most of the daily energy used in our lives comes from non-renewable fossil fuels, which has led to serious air pollution problems<sup>[1]</sup>. As contemporary society uses fossil fuels and nuclear energy, renewable and cleaner energy sources, including wind, solar, hydro, biomass, geothermal and others, are sought and investigated, propelling energy conversion and storage technologies<sup>[2-4]</sup>. Clean electrochemical energy storage is a highly effective method for storing and transmitting energy as a strategy of energy utilization. The importance of energy storage technology is rising. As energy storage is a vital aspect of modern life, experts have been studying various strategies for increasing its efficiency for decades<sup>[5-6]</sup>. Since SONY launched LIBs in 1991, rechargeable LIBs have become an indispensable energy storage device for portable electronic devices and electric vehicles<sup>[7]</sup>. This also continues to stimulate the growth and development of electronic gadgets and alternative-energy vehicles. Lithium metal is an ideal anode because of its high theoretical specific capacity of 3 860 mAh g<sup>-1</sup> and low electrode potential of -3.04 V with respect to hydrogen electrodes<sup>[8]</sup>. Existing mature technologies of LIBs with graphite anodes and

lithium transition metal oxide (LTMO) cathodes may attain a specific energy of 250 Wh kg<sup>-1</sup>, and the energy density would grow to 440 Wh kg<sup>-1</sup> if the anode is replaced with Li metal anode. This occurrence demonstrates the benefits of lithium metal as an anode based on a continuous plating/stripping mechanism that contributes to a higher energy output than conventional commercial anodes<sup>[9]</sup>. Owing to their low costs, LMBs are frequently employed in mass manufacturing, and their commercialization continues to be in progress.

However, the research and development path of LMBs have so far faced many obstacles and challenges<sup>[10]</sup>. LMBs have the following main issues in practical applications: (1) High chemical reactivity. This characteristic can cause lithium metal and electrolyte to interact and react, causing a continual decrease in the CE and poor electrochemical performances of the cells. (2) Susceptible lithium dendrites. Uneven Li<sup>+</sup> distribution will inevitably produce lithium dendrites. Short circuits, thermal runaway and a number of other problems can be caused by lithium dendrites. (3) Significant volume variation. Frequent plating/stripping of uneven lithium at the electrodes can lead to the creation of dead lithium and stacking, leading to structural instability<sup>[11-13]</sup>. On the basis of

**Received date:** 2023-02-15; **Revised date:** 2023-03-23

**Corresponding author:** GAO Xuan-wen, Ph.D, Associate Professor. E-mail: gaouxuanwen@mail.neu.edu.cn;  
LUO Wen-bin, Ph.D, Professor. E-mail: luowenbin@smm.neu.edu.cn

**Author introduction:** CHEN Yue<sup>†</sup> and ZHAO Lu-kang<sup>†</sup> contributed equally to this work

these electrochemical reaction features, researchers have determined that the severe issues of the LMA may be effectively solved by developing a protective layer on its surface<sup>[14]</sup>, building a 3D porous host<sup>[15]</sup>, synthesizing the various artificial solid-electrolyte interphase (SEI)<sup>[16]</sup>, and regulating ion deposition<sup>[17]</sup>. Although extensive researches have been carried out to inhibit the growth of lithium dendrites, it should be noted that a single method cannot solve all the problems of LMA<sup>[10,18]</sup>. SEI could improve CE and inhibit dendrite formation because it controls the side reactions between Li and the electrolyte in a good way<sup>[19-21]</sup>. Even though a well-functioning SEI can be a key part for keeping electrolyte solutions from decomposition in batteries<sup>[22]</sup>, we still don't know for sure which parts of SEI are the most important for keeping electrolytes from decomposition<sup>[23-25]</sup>. Consequently, more study of the electrode-solid electrolyte interface is necessary, and the solid surface electrolyte remains a substantial hurdle to the development of LMBs<sup>[26-28]</sup>. Further, since LMA does not require a host, it is possible that this method may fail under infinite volume variations when applied to carbon-based materials for the artificial creation of SEI<sup>[29]</sup>. In a lithium metal battery, Li<sup>+</sup> in the electrolyte react with the electrode material at the electrode surface to carry out the charging and discharging process. In LMBs, Li<sup>+</sup> in the electrolyte react chemically with the electrode material on the electrode surface for the charging and discharging process. When charging, Li<sup>+</sup> enter the electrode material from the electrolyte forming lithium metal deposited on the electrode surface; when discharging, lithium metal dissolves from the electrode surface into Li<sup>+</sup> and returns to the electrolyte. This process is reversible, but in actual use, there are some problems. A major problem is that the uniformity of lithium deposition on the electrode surface is poor. Due to the differences in the geometry and chemical activity of the electrode material surface, the distribution of Li<sup>+</sup> on the electrode surface is not uniform, which easily leads to local deposition of Li<sup>+</sup> on the electrode surface. This local deposition can lead to local volume expansion of the electrode material and even problems such as lithium dendrite growth, which can seriously affect the electrochemic-

al performance and safety of the battery. Carbon materials could help to regulate the homogeneity of lithium deposition, mainly through the following: (1) Excellent electronic conductivity. The excellent conductivity of the carbon-based framework provides a path for electron transport and facilitates the uniform deposition of Li<sup>+</sup>. At the same time, the higher specific surface area homogenizes the Li<sup>+</sup> flow and avoids the uneven deposition due to the local uneven current density. (2) Excellent mechanical stability. Carbon materials have high mechanical stability and can resist the volume expansion and contraction caused by Li<sup>+</sup> deposition. As Li<sup>+</sup> deposition would lead to volume expansion of the electrode, and poor mechanical stability of the electrode material would lead to deformation and fracture of the electrode structure. The carbon material has better mechanical stability, which can reduce the volume deformation of the electrode material, maintain the stability of the electrode structure, and keep the cycle life and energy density of the battery<sup>[9,30]</sup>.

Currently, it is believed that homogenous plating/stripping and the generation of minimal nucleation overpotentials are conceivable due to the rational design of the 3D skeleton structure with large specific surface area and strong structural stability. Porous scaffolds are an effective way to reduce current density and accommodate volume expansion, as a result of their high specific surface area and the enough space to host lithium metal<sup>[31-33]</sup>. So improving the stability and safety of LMBs through the selective use of porous collectors is a useful method that is gaining attention in research activities<sup>[34-35]</sup>. Porous 3D collector could effectively increase energy density. Among various 3D scaffolds, metal-based materials, which includes 3D copper-based collectors<sup>[36-37]</sup>, 3D porous CuZn collectors<sup>[38]</sup>, nickel foam collectors<sup>[39-40]</sup> and other porous metal structures, have been extensively investigated as the main matrix of lithium metal. Traditional metal 3D collectors could also stop dendrites from growing, but the large size and high density of the metal make it hard to deposit evenly on the lithiophilic surface during the whole reaction. These drawbacks lower the specific capacity of Li anode<sup>[41-44]</sup> and

application possibility in real life or manufacturing. As a well-established class of anode materials for LMBs<sup>[15, 45]</sup>, carbon materials are widely used and studied in LMBs because of their good electronic conductivity, low density, multiple functionalities, low cost, high lithium storage capacity, high specific surface area, excellent chemical stability, high mechanical strength and controlled structure<sup>[46-48]</sup>. Considering the recent significantly process have gained in carbonaceous scaffolds, this thesis focuses on a review of the advanced applied strategies in stabilizing LMA improving electrochemical performance. As shown in Fig. 1, it is mostly talked from the point of view of pure carbon-based materials, carbon-based materials with elemental metal composites, carbon-based materials with metal compounds (like metal sulfides, metal nitrides, metal oxides, metal phosphides, metal carbide and so on). This research looks at how various carbon-based scaffold composite lithium electrodes behave as current collectors for better lithium metals, with a particular emphasis on how the  $\text{Li}^+$  deposit on the surface of the material. It helps to promote the development of LMBs and learn more about how the structure and performance of composite lithium electrodes in carbon-based material scaffolds are

related. It presents a rational concept that may be used in the upcoming days for the creation of carbon-based lithium metal current collector materials.

## 2 Carbonaceous scaffolds

Graphene material, which is made of carbon, offers the benefits of being lightweight, having a low density, and being simple to produce. It has been proven that using graphene as a porous collector for LMBs may enhance the total energy density<sup>[49-51]</sup>. Due to its two-dimensional structure, the formation of lithium dendrites and the production of dead lithium can be prevented, which expands to accommodate lithium stripping/plating throughout the reaction. Its abundant functional groups can also guide the nucleation and deposition of  $\text{Li}^+$ <sup>[49, 52]</sup>. This technique can improve the stability of LMBs by reinforcing the connections at their interfaces.

Due to the easy modification of graphene, the introduction of heteroatomic doping becomes an effective means of guiding the homogeneous deposition of lithium metal at the reaction interface<sup>[49, 53]</sup>. Most additional heteroatoms have lithiophilic properties, which reduces the nucleation overpotential of  $\text{Li}^+$  on the surface of lithium metal to a large extent. This makes lithium deposition more even and less clumpy<sup>[54-57]</sup>. Heteroatoms alter both the qualitative and electronic characteristics of carbon materials, making them ideal for energy storage<sup>[58-59]</sup>. Graphene oxide (GO) is a particular monolayer of graphite oxide that contains several different oxygen functional groups<sup>[53]</sup>. GO can be obtained chemically from graphite and is widely available at low costs. It has been shown that GO materials have many excellent properties, such as easy processing, good mechanical strength, high ionic conductivity and excellent flexibility<sup>[60-61]</sup>. In addition, GO has good electrical insulation properties and a strong surface modification capability<sup>[62-64]</sup>. Yang's team<sup>[65]</sup> prepared a GO porous framework by 3D printing, which could adsorb molten lithium as a highly reversible lithium anode. The organized microchannel and microcavity structure of 3D GO within the skeleton is able to limit the dendrite development and

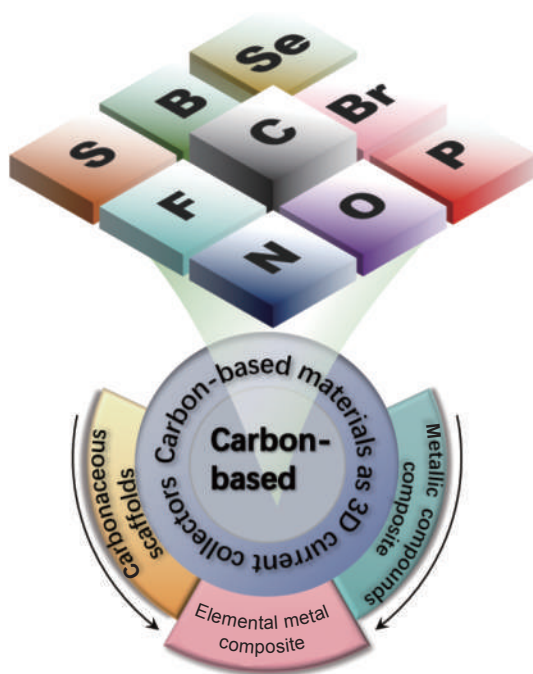


Fig. 1 Carbon-based materials in LMBs as 3D current scaffolds

handle a significant quantity of lithium deposition. This 3D-GO skeleton has a smaller mass due to its main body being carbon-based. Because the skeleton has a large specific surface area, the actual current density is decreased. This makes the cycle more stable by reducing the negative effect on the real specific capacity of the lithium cathode. The graphene oxide porous framework modification strategy provides a trustworthy strategy for achieving stable and high-energy density LMBs. In addition to the exceptional features of oxygen-doped 3D graphene, substantial research has also been conducted on S-doped 3D graphene. S-doped carbonaceous materials improve the conductivity of primary structural LMBs and boost polysulfide chemical reactivity<sup>[59]</sup>. Li et al.<sup>[66]</sup> prepared sulfur-doped 3D graphene/sulfur particle (S-3DG/S) high-sulfur composites by a one-pot wet chemical process. As shown in Fig. 2a, after the GO was treated using  $\text{NaHSO}_3$  the sulfur content was modified from 60% to 80% (mass fraction) through changes of sodium sulfide ( $\text{NaS}_2$ ) concentration. S is added to the 3DG/S framework at a concentration of 1.8% by weight. The porous structure consists of many interconnected channels, which aid in both material movement and polysulfide containment. S-doping improves attraction and junction energy of non-polar carbon particles with polar polysulfides. Adding S to graphene boosts its electrical conductivity, making it a more effective electrochemical material. Recently, the insertion of N atoms into the carbon base for materials has been intensively explored to promote the uniform deposition of lithium in LMBs and improve the performance of lithium metal<sup>[67-69]</sup>. Fang's team<sup>[70]</sup> used graphene as a substrate to synthesize N-doped CNTs. Utilizing N-doped carbon nanotubes (NCNT) to change the 3D graphene substrate considerably enhances the specific surface area. The enhanced specific surface area decreases the current density of lithium plating and preserves the integrity of the electrode structure, hence creating favorable circumstances for the final homogeneous lithium plating and eventually combining with lithiophilic N-functional groups to efficiently direct lithium deposits to nucleate evenly, limiting the form-

ation of lithium dendrites, and increasing the lifespan of LMBs. Huang's team<sup>[71]</sup> developed 3D nanoporous graphene (Fig. 2b), this material is comprised of graphene sheets with a 3D bicontinuous nanostructure that are coupled in a seamless manner. Additionally, a nanoporous nickel-based chemical vapor deposition (CVD) technique was used to construct a 3D nanoporous N-doped graphene matrix. The fit in Fig. 2c shows 3 peaks, indicating pyridine, pyrrole and quaternary nitrogen. These N-doped functional groups are lithiophilicity and adhere to the graphene surface, providing more uniform nucleation sites and a smaller nucleation overpotential than the copper foil surface. The main N-doped functional groups in the NG framework and N-doped graphene-enhanced Li anodes are pyridine nitrogen and pyrrole nitrogen, which exhibit remarkable cycling stability and multiplicative properties. Zhang's team<sup>[72]</sup> utilized an N element-doped graphene coating on the inner surface of porous copper for boosting the uniform deposition of Li (Fig. 2d), which influences the establishment of a stable SEI. Since N-doped graphene encourages Li to be deposited uniformly on the collector, the electrochemical performance was improved significantly. Because of the unique structure of graphene, electrons near the collector surface tend to be equally dispersed after lithium plating on N-doped graphene. Strong interactions between  $\text{Li}^+$  and N-doped graphene lead to a uniform flow of  $\text{Li}^+$ , which could lead to a uniform deposit of Li. The above statements indicate the superior characteristics of N-doping. Qiao et al.<sup>[73]</sup> constructed N-doped carbon nanotube-modified carbon cloth (NCNT-CC) as a 3D current collector. On the surface of carbon cloth (CC), N-doped carbon nanotubes were grown to produce stable 3D LMA. A 3D skeleton of N-doped carbon nanotubes on CC was obtained by catalytic growth of CC in a dicyandiamide atmosphere with carbonized  $\text{Co}^+$  (Fig. 2e). When carbon nanotubes are present, the specific surface area of CC goes up. This means that the local current density goes down. N doping significantly improves the lithiophilicity of the NCNT-CC backbone, induces Li homogeneous nucleation, inhibits the in-

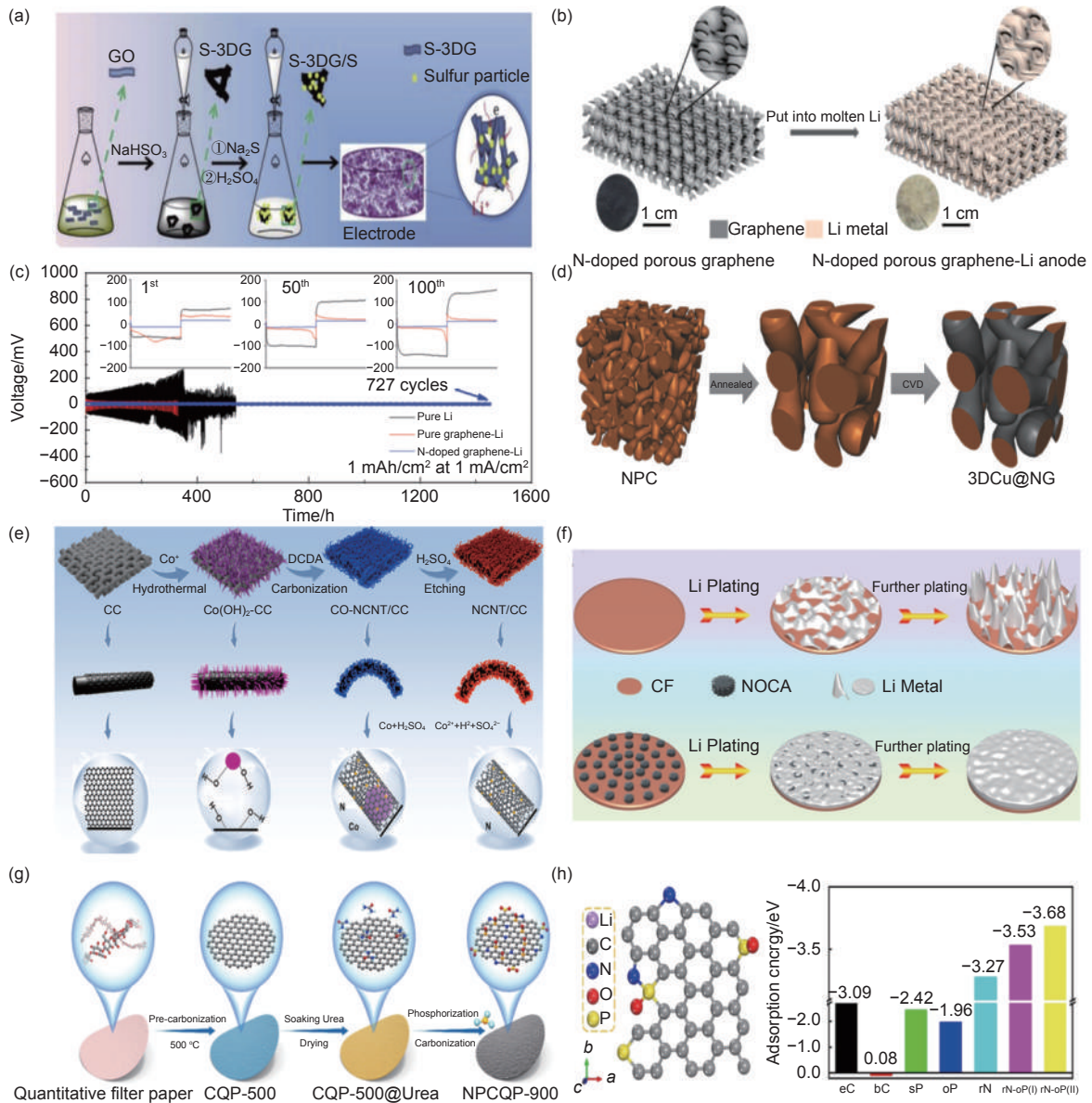


Fig. 2 (a) Schematic diagram of the production steps of S-3DG/S and the transmission path and framework of Li and electrons<sup>[66]</sup>. (b) Schematic of LMA: nanoporous N-doped graphene synthesis<sup>[71]</sup>. (c) Li foil, graphene-Li, and N-doped graphene-Li symmetrical cells with  $1 \text{ mA cm}^{-2}$  stripping/plating capacity and  $1 \text{ mA cm}^{-2}$  current density and voltage characteristics<sup>[71]</sup>. (d) Schematic diagram of 3DCu@NG manufacturing<sup>[72]</sup>. (e) The production steps of the NCNT-CC film<sup>[73]</sup>. (f) Schematic diagram of the deposition behavior of lithium deposition on CF and NOCA@CF<sup>[75]</sup>. (g) Schematic diagram of the NPCQP-900 synthesis process<sup>[76]</sup>. (h) Adsorption energy doped with carbon and lithium atoms<sup>[76]</sup>. (Reprinted with permission)

homogeneous formation of Li dendrites, and provides excellent stability and reversibility during cycling. The NCNT-CC electrode battery maintained a high CE of 99.67% after being tested at  $1 \text{ mA cm}^{-2}$  and  $1 \text{ mAh cm}^{-2}$ , which is a substantial improvement over the previous battery design. Boron has gotten a lot of attention as a possible anode for the next generation of high-energy rechargeable batteries. Electrochemical inertness inhibits the boron anode as a result of the high covalent bond aggregation in the boron skeleton,

resulting in the failure of the boron anode to be applied on a large scale in actual batteries. To solve this problem, Wang's team<sup>[74]</sup> obtained a porous graphene-based framework by limiting the quantum-sized B-spot to the surface of reduced graphene oxide. The quantized boron point (BQD) is synthesized and inserted in the conductive graphene matrix to construct a 3D cross-linked BQD/reduced GO (B@rGO) skeleton. In order to increase electrochemical performance, the 3D cross-linked conductive structure activates the

BQD to reversibly store and release lithium, which in turn efficiently maintains the alloy reaction, preserves the anode structure, and prevents the aggregation of active boron.

Single-atom doping strategies have led to a plethora of strategies in carbon-based materials, while heteroatom doping has been successful in improving the lithophilicity of carbon, the synergistic impact of heteroatom double doping on the lithophilicity of carbon has not been exhaustively studied<sup>[77]</sup>. At present polyatomic co-doping is also widely studied, and on the basis of single-atom doping, bipolar doping of heteroatoms in carbon materials is further proposed<sup>[78–79]</sup>. An's team<sup>[75]</sup> explores N/O double-doped carbon arrays (NOCA@CF) grown tightly on copper foam as a stable scaffold for lithium metal anode. High N/O double doping improves hydrophilicity and lithophilicity, which help induce homogeneous Li metal deposition and inhibit metal dendrite growth. As shown in Fig. 2f, the Li metal deposition morphology on CF and NOCA@CF using an ether-based electrolyte at  $1 \text{ mA cm}^{-2}$ , it was found that NOCA@CF was much more uniform than CF lithium deposition, effectively inhibiting dendrite growth. The large surface area contributed by the NOCA layer reduces the local current density and facilitates the induction of a uniformly distributed electric field. NOCA@CF, produced by a simple binary solvent process, exhibits low density, outstanding hydrophilicity and lithophilicity, high electronic conductivity, a large specific surface area and structural stability. The team of Gao<sup>[80]</sup> has doped N and O elements in hollow carbon nanospheres (NOCS) as a collector for LMA. Studies have shown that NOCS as an anode collector could improve the CE and stabilize the cycling performance of batteries. Large lithium metal deposits may be accommodated inside the NOCS, lowering the local current density and limiting the production of lithium dendrites. Lower voltage hysteresis and a longer cycle life are produced due to a more stable and homogeneous Li plating/stripping process on the NOCS electrode. In summary, pyrrole-N, carboxyl-O, keto-O and epoxy-O have favorable binding energies for Li atoms and

may considerably increase the Li affinity of NOCS electrodes and stabilize Li deposition and dissolution. New possibilities are offered for the realistic development of LMA. As the main body of a LMA, Lu et al.<sup>[76]</sup> put forward a N, P double-doped carbon (NPCQP) acquired through quantifying filter paper. The final product of NPCQP-900 is made from the precursor of NPCQP by nitriding and phosphating (Fig. 2g). As shown in Fig. 2h, the adsorption energies of C and pyrrolic N site (rN) are much higher than those of edge side of C atom (eC), while the adsorption energies of P-doped eC are lower than those of eC, indicating less Li adsorption capability. Nevertheless, Li adsorption capability at the two points of the rN and P-O (rN-oP) bridge site shows an ultra-high adsorption energy for Li atoms, suggesting that the double doping of N and P could synergistically enhance the lithophilicity of the carbon framework. Doping N and P heteroatoms could give lithium a lot of active sites to form nuclei, improve the nucleation mode of lithium on carbon substrates, and make it easier for lithium to be plated or stripped on carbon substrates.

To understand how dopant interactions affect carbon lithophilicity. Tang's team<sup>[81]</sup> prepares a 3D skeleton (NSC@Ni) composed of N and S co-doped carbon-covered nickel foam. By using an interfacial polymerization method and following carbonization stage, a carbon film co-doped with N and S is uniformly coated on the nickel foam surface (Fig. 3a). N, S co-doped carbon significantly enhances the lithophilicity of NSC@Ni. As shown in Fig. 3b, when both N and S elements are embedded into the carbon material, the  $E_a$  values of PIN-S and PdN-S become more negative than those of PIN and PdN, indicating enhanced interaction with Li atoms and that NSC@Ni could act as a homogeneous Li deposition. Carbon-based 3D collectors and lithium metal cathodes have been investigated extensively. In addition to the aforementioned methods, such as compounding with metal compounds, we have found many other forms of carbon-based structural energy storage. Chen et al.<sup>[82]</sup>

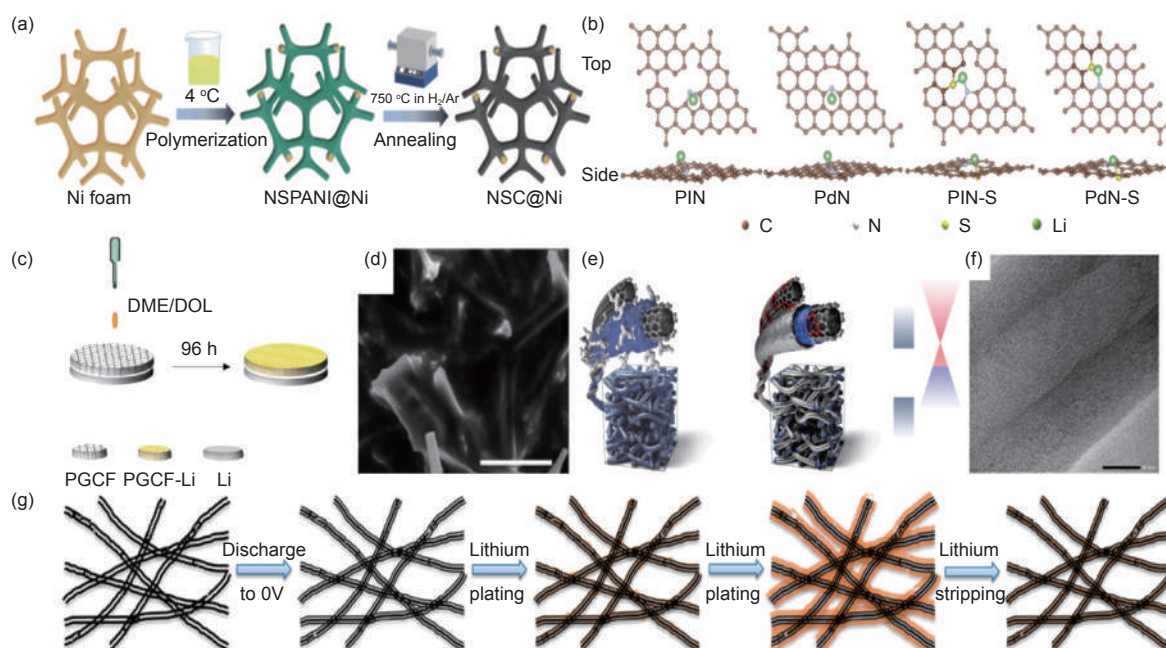


Fig. 3 (a) Graphical depiction of the NSC@Ni synthesis method<sup>[81]</sup>. (b) Optimal configuration of lithium atoms adsorbed at PIN, PdN, PIN-S and PdN-S sites<sup>[81]</sup>. (c) The fabrication process of PGCF-Li<sup>[82]</sup>. (d) The SEM image of PGCF-Li is  $10 \text{ mAh cm}^{-2}$ <sup>[82]</sup>. (e) Dual-function schematic diagram of a carbon surface with an electron-deficient structure<sup>[83]</sup>. (f) Physical characterization of the CNT sponge in HRTEM images<sup>[84]</sup>. (g) Morphology of carbon nanotube sponge during lithium plating/stripping: schematic representation of lithium discharged to carbon nanotube sponge's electrochemical plating/stripping process<sup>[84]</sup>. (Reprinted with permission)

prepared ultra-high porosity graphitic carbon foams by carbonizing melamine at a suitable temperature, and then obtained partially lithiated graphitic carbon foams (PGCF-Li) by uniformly distributing Li on the partially graphitic carbon foams (PGCF) *via* a C-Li intercalation reaction (Fig. 3c). On the one hand, the graphite intercalation compounds of Li (GICs-Li) have an excellent Li affinity and thus induces homogeneous Li deposition. On the other hand, the 3D porous graphitic carbonated foam has a high specific surface area as well as a high porosity, both of which provide routes for the movement of  $\text{Li}^+$  while also lowering the current density. As illustrated in Fig. 3d, the entire framework of PGCF is filled with Li when plated at a current density of  $10 \text{ mAh cm}^{-2}$ , after which the Li of the raw carbon skeleton can again be seen to be stripped out before slowly disappeared during the stripping process, indicating that PGCF-Li facilitates a reversible plating/stripping process. Kwon's team<sup>[83]</sup> investigated a multi-spin defect enrichment in carbon as an anode collector for LMBs. The carbon layers with multivacancy (MV) defects were selected

by coating them with graphite on commercial carbon paper to give them a defective structure. As shown in Fig. 3e, this demonstrates that the MV defect is responsible for the strong binding of the adsorbed atoms of Li. This is accomplished by limiting electron transport to the electrolyte's LUMO. This allows countless lithium cores to blossom laterally on the surface of the current collector and evenly distribute the lithium. The completely lithiated MV defects act as nucleation sites due to their lipophilic properties, preventing the surface diffusion of Li nucleation from aggregating. Huang et al.<sup>[85]</sup> utilized vertical graphene (VG) films grown on graphite paper (GP) as an all-carbon collector to regulate uniform Li nucleation and inhibit dendrite growth. Lithium deposition can be further guided by the lithiation reaction between graphite paper and lithium metal, which helps to improve the lithophilicity and reduce the lithium nucleation potential and overpotential. Yang et al.<sup>[84]</sup> uses carbon nanotube (CNT) sponges as 3D scaffolds for lithium deposition. CNT sponges that are available on the market are used as 3D collectors for dendrite-free lithium metal depos-

tion in LMBs so as to improve the CE of these batteries as well as their cycle stability. The pre-lithiation characteristic of porous CNT enhances its attraction for deposited lithium, while its high specific surface area boosts the quantity of lithium nucleation sites and ensures uniform lithium deposition. As illustrated in Fig. 3f, the existence of a rather thick interference border suggests the graphene layer arrangement of the CNT partition. The above plating/stripping process on CNT sponges is summarized as shown in Fig. 3g. The  $\text{Li}^+$  present in the CNT interlayer are adsorbed on the CNT surface to offer a lithophilicity characteristic, and the deposited lithium atoms nucleate on the covering, resulting in a low nucleation potential. The great firmness of the deposited lithium metal in the ether-based electrolyte and the suppression of lithium dendrites on the CNT sponge guarantee high CE and a high cycle stability for lithium plating/stripping. These results illustrate the possibility of using CNT sponges as 3D porous collectors for lithium deposition and have important implications for the invention and improvement of improved lithium electrode collectors. As shown in Table 1, the performance of some carbonaceous scaffolds as 3D current collectors for LMBs is summarized.

### 3 Elemental metal composite

Despite the advancements in the evolution of 3D bare carbonaceous scaffolds, the uneven mass and charge transfer at their interface with the electrolyte still results in an isolated and random distribution of  $\text{Li}^+$  nucleation sites on the surface of the collector flu-

id, thus promoting the creation of lithium dendrites<sup>[86-88]</sup>. However, it has been shown that carbon based materials composite with metal monomers can improve the lithophilic properties of the matrix material<sup>[89]</sup>. Ag nanoparticles (AgNPs) are often used as heterogeneous crystalline species for Li nucleation because of the good solubility of Ag in lithium<sup>[90]</sup>. Yang et al.<sup>[91]</sup> used joule heating to prepare ultrafine AgNPs that are evenly and securely attached to carbon nanofibres (CNFs) to promote lithium deposition. As illustrated in Fig. 4a, the AgNPs are dispersed equally across the carbon fibers to create a sturdy 3D structure. Ag acts as a nucleation site to selectively nucleate Li on the AgNPs to develop an alloy, then Li continues to be deposited on the Ag NPs, and finally, due to the induction of Ag, Li is deposited on the substrate of CNFs forming a smooth and uniform Li layer without the formation of Li dendrites. Sun et al.<sup>[92-93]</sup> also used a salt-assisted polymer foaming method to change AgNPs on 3D multi-N-doped carbon nanosheet structures. This strategy was employed to improve the lithophilic nature of the carbon-based material. The deposition behavior of  $\text{Li}^+$  was controlled by the lithophilic nature of the N-containing components of the carbon matrix (pyridine nitrogen, pyrrole nitrogen and graphite nitrogen). The 3D porous negative electrode material (3D-AGBN) with binary mesh layering (Fig. 4b) was formed by Xue et al.<sup>[94]</sup>, this 3D GO composited with Ag nanowires (AgNW) exhibited excellent multiplicative performance and cycling stability. Porous or nanostructured materials have a very large specific surface region,

**Table 1 Performance of LMBs using carbonaceous scaffolds as 3D current collectors**

Current collector	Half cell performance (Cycle Number/h, CE)	Operating conditions (Current density/(mA cm <sup>-2</sup> ), Areal capacity/(mAh cm <sup>-2</sup> ))	Refs
3D-printed GO frameworks	300, 95.5%	1, 1	[65]
Sulfur doped 3D graphene/sulfur particles	100, 93.9%	0.5, 1	[66]
N-doped graphene modified 3D porous Cu	50, 97.0%	1, 2	[72]
N-doped carbon nanotube modified carbon cloth	400, 99.7%	1, 1	[73]
N/O dual-doped 3D porous carbon	350, 95.7%	1, 1	[75]
N, P dual-doped carbon	200, 97.5%	1, 1	[76]
3D N, O co-doped carbon nanosphere	600, 98.2%	0.5, 0.5	[80]
CNT sponge as a 3D porous	90, 98.5%	1, 2	[84]

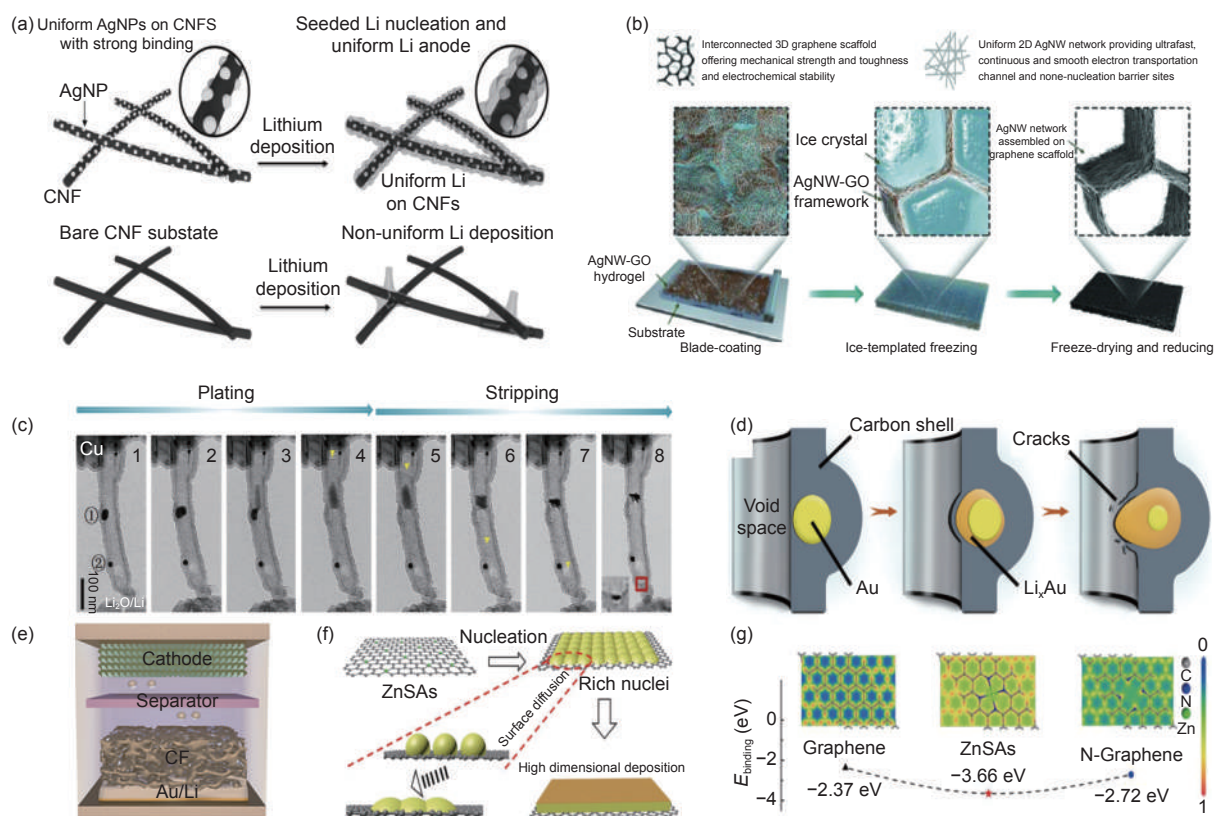


Fig. 4 (a) A diagrammatic representation of the nanoseeding approach for the homogeneous deposition of lithium metal on a 3D host material Joule heat anchors AgNPs evenly to the CNF substrate, which is responsible for Li deposition and growth. Thus, lithium metal is guided into the 3D substrate to generate a homogeneous lithium anode<sup>[91]</sup>. (b) Schematic diagram of the 3D-AGBN host preparation process with the layered characteristics of the solution<sup>[94]</sup>. (c) The Li plating/stripping process within the Au@aCNT is shown in the TEM snapshot and the corresponding schematic<sup>[96]</sup>. (d) Schematic of embedded AuNP entering the interior of the tube by breaking through the separation layer upon lithiation<sup>[96]</sup>. (e) Li is directed deposition to the bottom of the Li/AuCF anode<sup>[97]</sup>. (f) Formation of multi-dimensional structures through deposition of single Zn atoms<sup>[98]</sup>. (g) A Schematic representation of the difference in electron density and surface binding energy between graphene, ZnSAs, and N-graphene<sup>[98]</sup>. (Reprinted with permission)

lowering the local current density and resulting in a uniform distribution of  $\text{Li}^+$  flux on the negative coating. At the same time, Ag shows a very low nucleation potential and acts as a non-uniform nucleation site for  $\text{Li}^+$ . Consequently, the spatial management of the lithium metal allows  $\text{Li}^+$  to be deposited in porous structure, thereby minimizing volume change during cyclic charging and discharging. Additionally, this layered structure preserves the mechanical strength and tensile strength of the overall electrode structure to survive the huge quantity of lithium deposited. Even under 10 C and 20 C discharge settings, the Li@3D-AGBN/NCM complete cell retains a discharge capacity of  $147 \text{ mAh g}^{-1}$  and  $116 \text{ mAh g}^{-1}$ , demonstrating outstanding stability.

In addition to Ag, Au has also been used to composite with carbon-based materials to form new com-

posite materials for stabilizing LMA. Nevertheless, a comprehensive understanding of the process of nucleation and its interaction with heterogeneous seeds in Li has yet to be established<sup>[95]</sup>. Lang et al.<sup>[96]</sup> embedded Au nanoparticles in amorphous CNT to form a cell system (Au@aCNTs) and directly observed the plating/stripping behavior of Au seed crystals Li and Na by *in-situ* projection electron microscopy (TEM). As shown in Fig. 4c, Au expands during early alloying with Li, at which point  $\text{Li}^+$  are deposited further along the carbon tubes around the Li-Au alloy, causing it to expand further in size to form lithium nuclei. The Li then grows up and down, which results that the Li nucleus and eventually fills the cavity of the carbon nanotube, at which point the Au is completely surrounded by Li as a crystalline species. However, there is no significant volume change in particle 2.

This is because there is a very thin layer of carbon between the Au particles and the inner tube where the Au is embedded (Fig. 4d). This coating of carbon restricts the increase of the mixture particles and slows the lithiation procedure. When the carbon layer is extremely thin, the carbon layer outer shell can break under severe pressure, which is the alloying process of Au particle 1. However, when this carbon layer is very thick or the Au particles are rather small, the Au particles are then firmly confined by the carbon layer, thus preventing the alloying of the Au particles and forming a “dead” particle such as particle 2. In addition, apart from being a crystalline species, Au can also be used to modify carbon fibers as 3D janus collectors due to its lithophilic nature. Due to low nucleation potential of Li as a forceful factor, Au can be manipulated to put  $\text{Li}^+$  on the bottom of carbon fibers<sup>[97]</sup>.

As depicted in Fig. 4e, the  $\text{Li}^+$  are deposited in a directional manner on the bottom of the anode, leaving a large space between the Li layer and the diaphragm, thus alleviating the problem of lithium dendrite formation. Additionally, the porous nature of the carbon fibers mitigates the issue of volume expansion when charging and discharging. Such a structure allows for both electrochemical stability and a lot of mechanical flexibility. This makes sure that the structure is stable and safe even when it is deformed.

Lower surface energy and a large diffusion energy barrier may lead to rapid growth of lithium dendrites during deposition<sup>[99–100]</sup>. Since single-atom materials sharply increase surface free energy, they are now also used to induce Li deposition at Li nucleation sites, and single atoms can provide a denser and more uniform deposition site to induce the formation of uniformly distributed Li layers<sup>[98]</sup>. Xu et al.<sup>[98]</sup> derived from first-principles calculations that Zn single-atom materials (ZnSAs) with high surface free energies and

low migration barriers are capable of inducing Li multi-dimensional deposition (Fig. 4f). Fig. 4g shows that ZnSAs-containing carbon carriers have a higher electron density and higher surface free energy than graphene. This means that ZnSAs have better electronic conductivity and a stronger ability to bind with  $\text{Li}^+$ . As shown in Table 2, the performances of some carbon-based materials composited with metal elements as 3D current collectors for LMBs are summarized.

#### 4 Composite with metallic oxygen/sulphur/selenium compounds

Since the affinity of a single carbon material and conductivity with lithium metal are not as strong as metals and metal oxides, researchers are becoming more and more interested in excessive metal oxides because they have high capacities, cheap and a lot of theoretical potential. The carbon-based material surface can be combined with other metallizations as a coating material for 3D fluidic framework due to its abundance of functional groups. So much research is currently being done using carbon-based materials and metal compounds for negative electrode modification.

Strong cross-linking between metal ions and polymer chains makes hybrids with a full carbon-bound structure. This is because carbon-based materials are very good at conducting electricity and transition metal oxides can store a lot of  $\text{Li}^+$  in theory<sup>[101–103]</sup>. As anodes, the engineering of transition metal oxides into 3D carbon networks promises a long cycle life and outstanding multiplier performance<sup>[104–105]</sup>. Xiang’s team<sup>[106]</sup> prepared an electrode configuration (CF@CNT/MgO) made of N-doped CF covered with CNT and adorned with ultra-small magnesium oxide nanoparticles (MgO NP). The introduction of a dense carbon nanotube cladding layer on the

**Table 2 Performance of LMBs using elemental metal composite as 3D current collectors**

Current collector	Half cell performance (Cycle number/h, CE)	Operating conditions (Current density/(mA cm <sup>-2</sup> ), Areal capacity/(mAh cm <sup>-2</sup> ))	Refs
Silver nanowire and graphene-based hierarchical host with a binary network structure	50, 97.3%	1, 6	[94]
Zn single-atom	250, 100%	1, 2	[98]

carbonaceous foam framework resulted in a highly conductive and robustly flexible hybrid. The ultrafine MgO NP modification and the ortho-N doped functional groups provided effective chemisorption of lithium polysulfide. This multifunctional complex improves the sulfur area loading and mitigates the shuttle impact in LSBs, increasing the capacity decay rate and providing high capacity retention of 68% after 350 cycles at 1 C. Zhang's group<sup>[19]</sup> developed a unique N-doped hollow carbon fiber (NHCF), carbon nanosheet (CN), and zinc oxide (ZnO) nanostructured skeletal substrate employing 3D fabric covered with 2-methylimidazole (2-MIZ) as a scaffold. The graded structure of this layered substrate and the presence of lithiophilic features create a stable environment for the plating/stripping of lithium metal. This keeps lithium dendrites from being made. Zhang et al.<sup>[107]</sup> proposed Al<sub>2</sub>O<sub>3</sub>-coated 3D carbon nanotube sponges (CNTS) as the main body for the deposition of Li. By using atomic layer deposition (ALD) technique, light, porous CNT with a large surface area was used as the skeleton material for depositing lithium, decreasing the current density efficiently, thus limiting the production of lithium dendrites. This innovative 3D CNT structure with a surface protection layer presents a novel approach for controlling the growth of Li dendrites and ensuring the stability of LMA for extended usage. Wang et al.<sup>[108]</sup> developed a carbonized metal organic framework (MOF) nanorod array-modified carbon cloth (NRA-CC) for homogeneous plating or stripping. The active Co and N atoms in the NRAs have lithium-loving properties that attract Li<sup>+</sup>, while the doped Co-core N atoms provide high electronic conductivity, which ensures a uniform Li<sup>+</sup> flux at the NRA-CC electrode surface. As shown in Fig. 5a, the development and volume expansion of Li dendrites during cycling causes the rupture of the SEI coating, and the deposition of Li<sup>+</sup> in the pitting holes could result in short circuits, thermal runaway, and long-term damage to the cell's structure. Due to the synergistic effect of the inter-linked CC and the homogeneous Co-N-C NRA, NRA-CC could act as an ideal body for Li plating/stripping. The carbonized MOF NRA ef-

fectively converts the CC from lithium sparse to lithiophilic, reducing polarization and ensuring homogeneous Li nucleation. 3D-interconnected CC and lithiophilic Co-N-C NRA synergistically promote homogeneous Li plating and improve anode durability at high areal capacity and current density, providing new ideas for the design of dendrite-free LMA for safe and secure solid-state LMBs. Yue et al.<sup>[109]</sup> constructed a lightweight, hollow 3D carbon skeleton using soybean oil as a raw material. The 3D structure of the carbon skeleton adjusts to the volume expansion of the electrode and governs the plating/stripping behavior, thereby inhibiting dendrite formation and the creation of dead lithium. Wetting of lithium can be enhanced by coating the surface of the 3D carbon skeleton with copper oxide. As depicted in Fig. 5b, the obtained Li composite electrode (OCCu-Li) was created by preparing a hollow carbon skeleton using CVD and then incorporating a copper oxide layer. The obtained OCCu-Li electrode has a high Li loading of 94% (mass fraction). The advancement of OCCu-Li electrodes for lithium-sulfur battery (LSB) is confirmed by the fact that they exhibit much lower overpotentials and much higher cycling stability than bare Li electrodes. Zeng's team<sup>[110]</sup> prepared ZnO nanosheets confined in N-doped carbon modified CC (CC@ZnO/NC). CC@ZnO/NC@Li was prepared by water bath deposition, annealing and fusion processes. The CC@ZnO/NC skeleton has a high Li affinity due to the synergistic effect of lithiophilic ZnO and N-doped carbon, achieving rapid infiltration of molten Li into the substrate to form a dense CC@ZnO/NC@Li composite anode. LiZn alloys obtained by the chemical reaction of ZnO and Li promote electron and ion diffusion and modulate Li in homogeneous coating and exfoliation, thereby inhibiting the deposition of Li dendrites. Xu et al.<sup>[111]</sup> prepared the lithiophilic porous flexible composite VO<sub>2</sub>-CNT/CNF by depositing VO<sub>2</sub> on a 3D-structured carbon network formed by CNF and N-doped CNT. As observed in Fig. 5c, N-doped CNT was grown on CNF fibers by a CVD process, followed by the deposition of VO<sub>2</sub> by PVD to form the VO<sub>2</sub>-CNT/CNF composite. The CNF provides

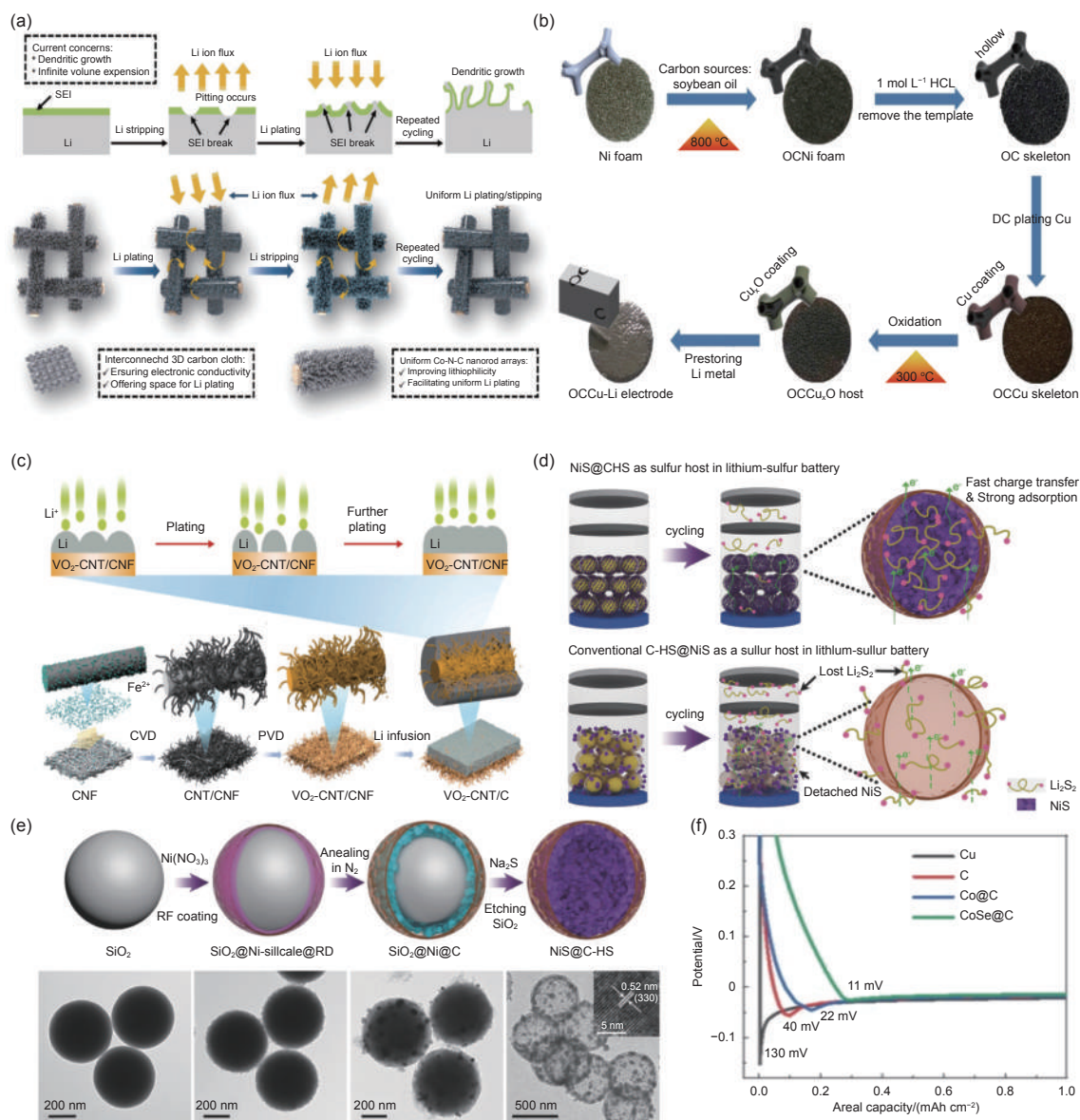


Fig. 5 (a) A diagrammatic representation of the peeling and electroplating behavior lithium foil in a planar form and Li@NRA-CC electrode, mechanisms of breakdown by pitting corrosion, SEI fracture, and dendritic growth, and it describes the synergistic influence of interconnected 3D CC and Co-N-C NRAs on lithium stripping/plating behavior<sup>[108]</sup>. (b) Process flow diagram for the production of OCCu-Li electrode<sup>[109]</sup>. (c) Schematic of synthetic procedures of VO<sub>2</sub>-CNT/CNF@Li electrode<sup>[111]</sup>. (d) Schematic diagram of the NiS@C-HS manufacturing process<sup>[112]</sup>. (e) Schematic of the sulfur hosts NiS@C-HS and typical C-HS@NiS<sup>[112]</sup>. (f) Voltage profiles during initial Li plating on different substrates at 1 mA cm<sup>-2</sup><sup>[113]</sup>. (Reprinted with permission)

abundant void space and microchannels for Li<sup>+</sup> deposition, which would buffer the volume changes during charging and discharging. Meanwhile, the N-doped carbon nanotubes grown on the CNF surface provided sufficient Li nucleation sites and reduced the local current density, thus inhibiting the growth of Li dendrites and achieving uniform Li deposition. VO<sub>2</sub>-CNT/CNF can make full use of its 3D porous surface to increase the lithium deposition sites and reduce the local current density. Moreover, the uniform distribu-

tion of VO<sub>2</sub> nanoparticles on CNT/CNF enhances their lithophilicity and facilitates the uniform deposition of Li<sup>+</sup>.

The abundant resources, low cost, and low toxicity of reactive sulfur materials give them great potential for practical applications. Strong pro-sulfur characteristics make metal sulfides an attractive sulfur host. Hybrids of metal sulfides and carbon can provide conductive scaffolds and high adsorption capacities for polysulfides and are already commonly

utilized as sulfur bodies in LSB. By using controlled simulation and uniformly distributed nano-sized nickel sulfide (NiS) on a 3D carbon hollow sphere (C-HS), Ye's team<sup>[112]</sup> created a 3D hybrid material (NiS@C-HS). As shown in Fig. 5d, NiS@C-HS was prepared by using NiS with SiO<sub>2</sub> nanospheres as hard templates, coated with benzophenone-4 formaldehyde, and carbonized in N<sub>2</sub>. As depicted in Fig. 5e, the assembly of Li-S cells with NiS@C-HS as the electrode shows the effect of a unique 3D hybridized sulfur body on the electrochemical performance, achieving a capacity of 695 mAh g<sup>-1</sup> after 300 cycles at 0.5 C. Similarly, metal-Se compounds have also been investigated. He's team<sup>[113]</sup> reports a 3D skeleton of CoSe nanoparticles coupled to conductive carbon nanowires (CoSe@C). Due to the higher electrical conductivity and excellent catalytic properties of CoSe, the 3D carbon aerogel modified with cobalt selenide nanoparticles (CoSe@C) as a dendrite-free LMA can direct the uniform growth of Li within the 3D skeleton and effectively inhibit the growth of Li dendrites. The high ionic conductivity of the Li<sub>2</sub>Se formed *in situ* during CoSe conversion facilitates rapid Li<sup>+</sup> diffusion and homogeneous Li plating/stripping. As shown in Fig. 5f, CoSe@C shows the lowest nucleation overpotential of 11 mV, demonstrating the strong lithophilicity of CoSe to greatly reduce the Li nucleation overpotential, which favors homogeneous Li deposition. As shown in Table 3, the performance of some carbon-based materials composited with metal oxygen/sulfur/selenium compounds as 3D collectors for LMBs is summarized.

## 5 Composite with metal nitrides/phosphides

Compared to metal oxides, metal nitrides have both a strong affinity for lithium and high ionic conductivity. Metal nitrides have a unique electronic

structure that makes them highly conductive, stable at high temperatures, and being good electrical conductors. The deposition of metal nitrides onto the surface of carbon carriers modulates the surface electron distribution by introducing additional coordination sites through the metal-nitrogen-carbon (M-N-C) structure. It has been used as a catalyst, refractory material, and coating in fusion reactors, as well as in various energy storage systems.

Gao's team<sup>[114]</sup> found that the combination of aluminum nitride (AlN) nanosheet additives and 3D carbon paper (CP) collectors significantly inhibited the growth of lithium dendrites and adapted to volume expansion. Calculations of the attachment energies between Li and different crystalline surfaces of Cu, CP and AlN nanosheets show that Li<sup>+</sup> have a higher binding energy to AlN compared to Cu and CP collectors. The calculated binding energies of Li<sup>+</sup> to AlN (100), (001) and (101) were 4.82, 3.15 and 3.88 eV, respectively (Fig. 6a), indicating that Li<sup>+</sup> are more favorably adsorbed on the surface of the AlN nanosheets at the interface between the Cu foil and the electrolyte, reducing collection and permitting easy diffusion and uniform distribution, resulting in dendrite-free Li deposition. Dendrite-free interface improves the electrochemical cycling performance of LMBs. Due to the reversible plating/peeling on the CP electrode, the CP electrode circulating in the additive electrolyte exhibits excellent electrochemical cycling performance that maintains a CE above 95.84% in 350 cycles at a current density of 1 mA cm<sup>-2</sup> (Fig. 6b). Nitride-modified nickel foam (PNNF) constructed by Zhu et al.<sup>[115]</sup>. Ni<sub>x</sub>N modified nickel foam (PNNF) effectively improves surface lithophilicity as a result of the chemical reaction with lithium forming Li<sub>3</sub>N and Ni, which leads to the uniform deposition of lithium on the PNNF surface, maintaining a homogeneous and

**Table 3 Performance of LMBs using composite with metallic oxygen/sulphur/selenium compounds as 3D current collectors**

Current collector	Half cell performance (Cycle number/h,CE)	Operating conditions (Current density/(mA cm <sup>-2</sup> ), Areal capacity/(mAh cm <sup>-2</sup> ))	Refs
Nanorod arrays modified carbon cloth	100, 97.5%	2, 4	[108]
Vanadium oxide modified carbon nanotube films	500, 99%	1, 1	[111]
3D carbon aerogel decorated with cobalt selenide nanoparticles	100, 99.3%	6, 6	[113]

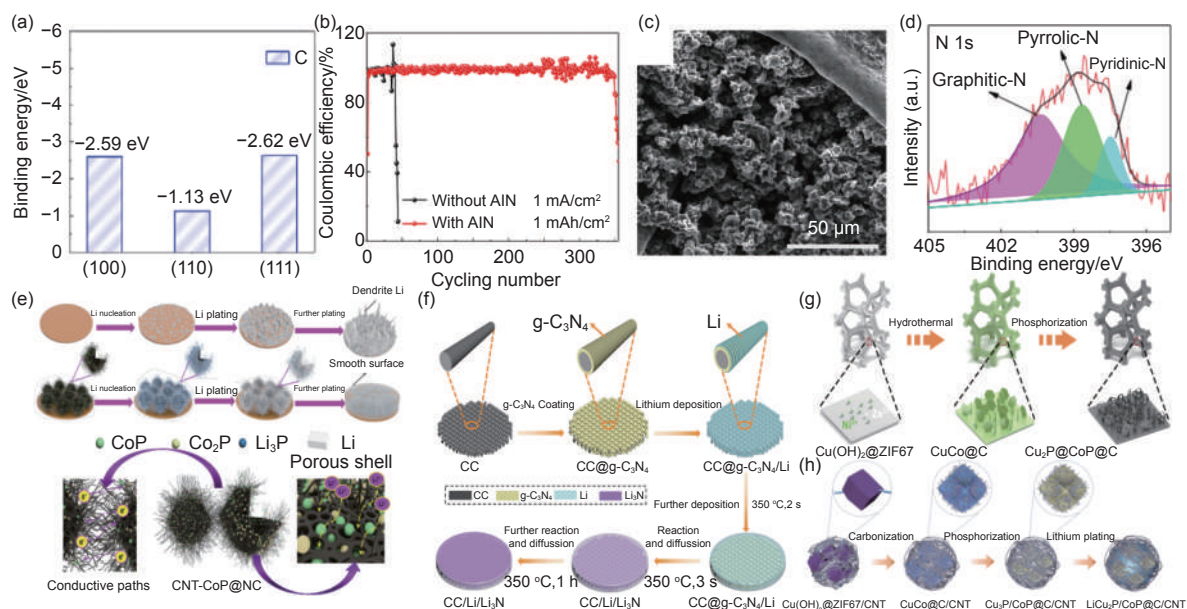


Fig. 6 (a) Describe the first-principles calculation of CP binding energy<sup>[114]</sup>. (b) CP electrodes CE at 1 mA cm<sup>-2</sup> and 1 mAh cm<sup>-2</sup> at different current densities and different capacities<sup>[114]</sup>. (c) SEM image of surface topography after Li@NF 100 cycles at 1 mA cm<sup>-2</sup><sup>[115]</sup>. (d) High-resolution XPS spectra of N 1s for CNT-CoP@NC<sup>[116]</sup>. (e) Lithium nucleation and electroplating process diagram on the Cu foil and CNT-CoP@NC electrode<sup>[116]</sup>. (f) Process diagram of the preparation process of the CC/Li/Li<sub>3</sub>N composite electrode<sup>[117]</sup>. (g) ZNP/NF synthesis process diagram<sup>[119]</sup>. (h) A diagrammatic representation of the preparation process of LiCu<sub>3</sub>P/CoP@C/CNT<sup>[120]</sup>. (Reprinted with permission)

compact morphology. PNNF not only inherits the microporous, 3D structure of NF but also has an enhanced specific surface area as a result of the presence of rough Ni<sub>x</sub>N layers. The Li@PNNF electrode displays a dense and smooth surface (Fig. 6c), demonstrating highly reversible lithium stripping/plating performances and greatly improved electrochemical performance. When combined with a LiFePO<sub>4</sub> (LFP) cathode, the Li@PNNF/LFP full battery demonstrates a high reversible capacity of 167.1 mAh g<sup>-1</sup> and outstanding multiplier performance after 300 cycles at 1 C. A new strategy for the stabilization of LMA by metal nitrides as a lithiophilic layer is offered. Song's team<sup>[116]</sup> meticulously developed carbon nanotubes (CNTs) covered with CoP/Co<sub>2</sub>P evenly dispersed N-doped hollow porous polyhedral carbon (CNT-CoP@NC) as a lithium metal matrix. As shown in Fig. 6d, the signals of pyridine N, pyrrole N and graphite N were found in CNT-CoP@NC. This shows that N doping and metal phosphide composite modification improved lithiophilicity, lowered the nucleation barrier, and led to uniform nucleation and stable deposition of lithium metal, which stopped the growth of lithium dendrites. The CNT-CoP@NC structure has

a large specific surface area and internal cavities, which further avoids the danger of volume expansion caused by lithium deposition. Fig. 6e, compares the Li plating process on bare Cu and CNT-CoP@NC electrodes, and the bare Cu foil forms an uneven nucleation that grows into large lithium dendrites. Cao et al.<sup>[117]</sup> prepared 3D lithium anode with gradient Li<sub>3</sub>N concentration *in-situ* fabricated on carbon-based framework by thermal diffusion method (denoted as CC/Li/Li<sub>3</sub>N). The energy barrier for Li<sup>+</sup> spreading on the Li<sub>3</sub>N layer is approximately 20 times lower than the energy obstacle on the Li surface. The entire fabrication process uses the thermal diffusion method (Fig. 6f), where the surface of the carbon-based skeleton is coated with g-C<sub>3</sub>N<sub>4</sub> on the in-situ CC and then a reaction occurs during the injection of lithium forming Li<sub>3</sub>N. Li<sub>3</sub>N promotes efficient diffusion of Li<sup>+</sup> and tolerates high current densities during the Li stripping/plating processes. The Li<sub>3</sub>N migrating to the upper surface would be uniformly dispersed throughout the 3D skeleton, which can reduce local current density, regulate uniform Li deposition, and eliminate the formation of Li dendrites. Luo et al.<sup>[118]</sup> put forward a 3D heterostructure composed of lith-

iphilic Mo<sub>2</sub>N homogeneously anchored in a carbon nanofiber (CNF) matrix by *in situ* reductive nitridation. Mo<sub>2</sub>N the strongly lithiphilic characteristic, evenly distributed in the Mo<sub>2</sub>N@CNF structure where acts as a pre-implanted nucleation seed to guide Li nucleation and deposition along the 3D framework. Meanwhile the high surface area of the CNF framework prevents Li deposition and slows the growth of Li dendrites.

In the same way, carbon-based materials and metal phosphide used in LMA could boost the performance of lithium metals. Owing to their strong lithiphilicity, conductivity and chemical stability, metal phosphides undergo favorable reactions with lithium. Lithium easily reacts with metal phosphides to form lithium phosphide, which has strong lithiphilic properties and improves the conductivity of Li<sup>+</sup>. Wang et al.<sup>[119]</sup> proposed a surface modification method for constructing nickel phosphide nanosheets (NZN/NF) on nickel foam. This approach significantly enhances the specific surface area of nickel foam, which not only gives an adequate nucleation site but also provides a substantial increase in surface area for helping to diminish the local current density to suppress lithium dendrites. Nickel phosphide could react with lithium to form Li<sub>3</sub>P, which has a high Li<sup>+</sup> conductivity to facilitate Li<sup>+</sup> transportation. As shown in Fig. 6g, NiZn layered hydroxide (NiZnLHS) was fabricated on nickel foam (NF) using the hydrothermal technique, and a NZN/NF nanosheet array was fabricated using the phosphation process. After multiple (100 cycles) treatment of NZN/NF, lithium is uniformly contained in the skeleton, making the position of lithium in the skeleton more uniform and dense. To achieve uniform lithium deposition, nickel-phosphide modified electrodes should be a better choice for ion

and electron transportation. Zhang et al.<sup>[120]</sup> synthesized rigid carbon nanocartridges containing Cu<sub>3</sub>P/CoP heterostructured nanobubbles. Compared to other samples, the surface of this carbon nanobox is covered with densely grown fluffy carbon tubes and carbon nanotube matrix that enhances the lithiphilicity and conductivity, contributing to an efficiently uniformed the Li<sup>+</sup> flux and the suppression of dendritic growth. After carbonization and phosphation, a multi-stage porous target Cu<sub>3</sub>P/CoP@C/CNT was successfully prepared using Cu(OH)<sub>2</sub> nanowires as the substrate to introduce carbon nanotubes (Fig. 6h). A close arrangement of Li with uniform and smooth surfaces was detected on top of Cu<sub>3</sub>P/CoP@C/CNT, and this dense and thinner deposited Li layer derives from the hierarchical 3D porous structure and lithiphilic effect of heterogeneous Cu<sub>3</sub>P/CoP and also demonstrates that Li atoms display a more robust bond energy, leading to dendrite prevention behavior during cycling. Cu<sub>3</sub>P/CoP@C/CNT exhibits good electrochemical performance and maintains a high CE (94.6%) at 0.5 mA cm<sup>-2</sup>/0.5 mAh cm<sup>-2</sup> for 220 cycles. As shown in Table 4, the performance of some carbon-based materials with composite with metal nitride/phosphide as 3D collectors for LMBs is summarized.

## 6 Composite with metal carbide

Mxene is a 2D carbide or carbon-nitride layered material with the general formula M<sub>n+1</sub>X<sub>n</sub>T<sub>x</sub>, where M is a transition metal component with  $n = 1, 2$  or  $3$ ,  $X$  is C or N, and T represents a terminal group such as O or OH<sup>[121-123]</sup>. It is now also widely used as an anode material for LMBs due to its good electronic conductivity, lithiphilic properties and mechanical stability<sup>[124-125]</sup>. Fang et al.<sup>[126]</sup> coated Mxene on car-

**Table 4 Performance of LMBs using composite with metal nitrides/phosphides as 3D current collectors**

Current collector	Half cell performance (Cycle number/h, CE)	Operating conditions (Current density/(mA cm <sup>-2</sup> ), Areal capacity/(mAh cm <sup>-2</sup> ))	Refs
Aluminum nitride nanosheets as an additive and carbon paper as 3D current collector	350, 95.8%	1, 1	[114]
Nitride decorated nickel foams	300, 97.0%	1, 3	[115]
Construction of nickel phosphide nanosheets modified with nickel foam	280, 98.5%	1, 1	[119]
Nitrogen-doped hollow porous polyhedron carbon	400, 96.9%	1, 1	[116]

bon cloth ( $\text{Ti}_3\text{C}_2\text{T}_x\text{-CC}$ ) to stabilize the 3D structure and induce the evolution of a favorable Li (110) lattice surface to stabilize the plating/stripping behavior of  $\text{Li}^+$ . In contrast to the bare Li electrode, the electrode surface remains smooth and free of Li dendrites even after several cycles and also forms a pebble-like bulk Li layer, which is identical to the Li deposition morphology on Mxene and dominated by the Li crystal surface (110), indicating a homogeneous deposition behavior on the Li (110) surface induced by  $\text{Ti}_3\text{C}_2\text{T}_x\text{-CC}$ . Furthermore, in order to examine further the impact of the crystal structure of Li on its electrochemical behavior, the kinetics and thermodynamics of Li crystal planes (110) were analyzed (200). The results show that the Li (110) crystal plane has a lower deposition energy (0.24 vs. 0.26 eV) and surface migration potential (0.02 vs. 0.16 eV), which also suggests that the Li (110) crystal plane is more conducive to Li diffusion and planar growth in two dimensions. The reaction mechanism is shown in Fig. 7a. The (200) crystal plane of the bare lithium electrode generates a lot of dendrites on the surface after long cycling, whereas the (200) crystal plane of the Li- $\text{Ti}_3\text{C}_2\text{T}_x\text{-CC}$  electrode transforms to (110) during cycling and initially forms a tight and homogeneous bulk lithium layer with no dendrite formation on the sur-

face.

Shi et al.<sup>[130]</sup> used aerogel synthesis to prepare highly conductive, lightweight Mxene/graphite (MG) Li metal skeletal structures. This arrangement takes advantage of large specific surface area of grapheme to increase Li loading, while the interconnected pore structure keeps it stable mechanically. Lithiophilic Mxene nanosheets, on the other hand, give Li a lot of places to start deactivating, which leads to even Li deposition and stops Li dendrites from forming. Even when put through 230 cycles of very high current densities, this flexible LMA has a very high CE of 99% throughout its entire life.

To solve the problem of low  $\text{Li}^+$  accommodation and low rates at high current densities in the 2D material Mxene<sup>[131]</sup>, Wang et al.<sup>[127]</sup> successfully prepared flexible MXene membranes as Li-body topologies by inducing the assembly of  $\text{Ti}_3\text{C}_2\text{T}_x$  MXene dispersions containing trace amounts of cellulose nanofibres (CNF) by spin evaporation techniques. The structural characteristics of this material are shown in Fig. 7b. CNF induces microsphere structures between Mxene sheets through intermolecular hydrogen bonding, thereby generating an interlocking structure between such microspheres and Mxene sheets to increase mechanical strength and toughness, which can

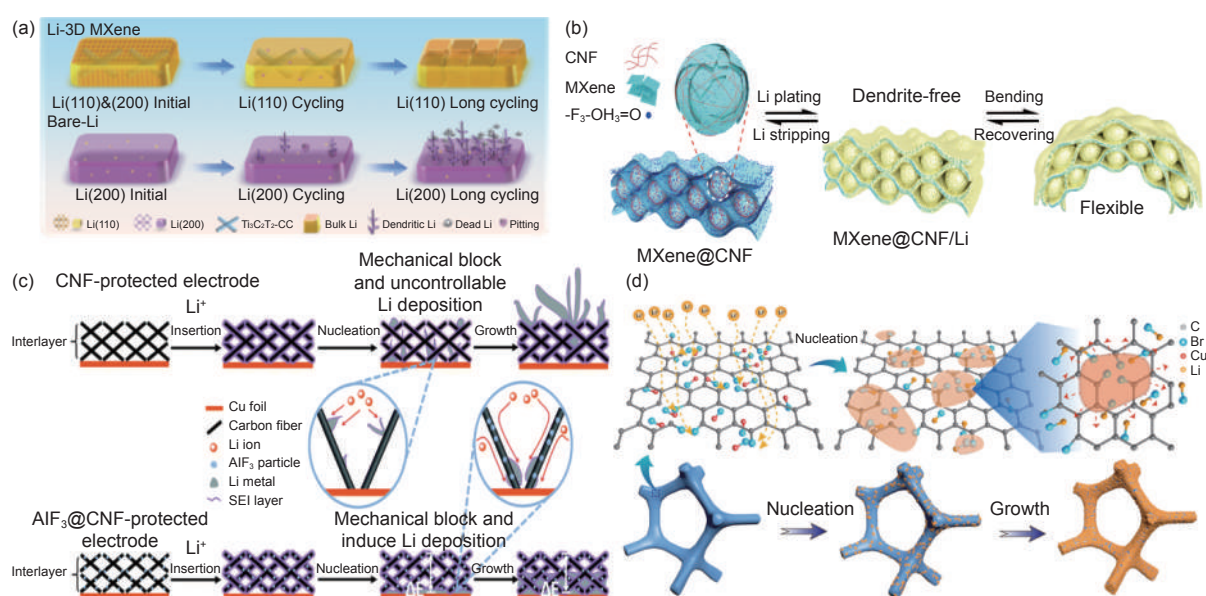


Fig. 7 (a) A diagrammatic representation of the reaction mechanism of Li- $\text{Ti}_3\text{C}_2\text{T}_x\text{-CC}$  with a bare lithium electrode<sup>[126]</sup>. (b) Diagram of lithium plating on MXene@CNF film<sup>[127]</sup>. (c) Schematic diagram of the lithium stripping/plating process of  $\text{AlF}_3$ @CNF interlayer. A potential gradient ( $\Delta E$ ) is formed as the resistance between layers increases<sup>[128]</sup>. (d) Schematic diagram of lithium metal deposition on BGCP<sup>[129]</sup>. ( Reprinted with permission )

recover even after bending. And also enhances the anode capacity of LMBs as a result of its high porosity. The MXene sheet has a number of lithiophilic functional groups and nucleation sites, rendering it lithiophilic, which produces homogenous Li deposition and increases the efficiency. XPS results reveal that in addition to the Li-reactive  $-\text{OH}$  and  $-\text{COOH}$  groups on the surface of MXene, there is also an inactive  $-\text{F}$  group that does not react with Li. However, the  $-\text{F}$  group can act together with the active group to produce uniform Li nucleation and growth by binding to  $\text{Li}^+$  through physical attraction. As shown in Table 5, the performance of some carbon-based materials with metal-carbide composites as 3D collectors for LMBs is summarized.

## 7 Composite with fluoride/bromide/iodide

In recent years, F and Br atom-doped carbon-based materials have also been shown to have strong lithiophilic properties, effectively inhibiting the growth of dendrites and extending the service life of lithium metal to boost security and stability. Guo's team<sup>[128]</sup> fabricated an  $\text{AlF}_3@\text{CNF}$  interlayer for the direct deposition of lithium in space in order to produce LMA with a long service life and dendrites free characteristic.  $\text{AlF}_3$  particles lower the nucleation overpotential of Li and control the electronic conductivity of the carbon interlayer to stop lithium from settling on the surface of the carbon interlayer.  $\text{AlF}_3@\text{CNFs}$  successfully limit the formation of lithium dendrites due to their high porosity, high elasticity, and high mechanical strength, which provide ample room to accommodate volume expansion. As shown in Fig. 7c, inhomogeneous Li aggregates and extends vertically beyond the CNFs, leading to dend-

ritic issues. Induced by  $\text{AlF}_3$ -modified nanofibres, Li metal tends to nucleate and proliferate near the interlayer base. As more Li is plated, metallic Li chunks progressively form and develop toward the top of the middle layer.  $\text{AlF}_3@\text{CNFs}$  achieved a high CE of 97.2% for 900 h in a carbonate-based electrolyte. LiF is widely used as a protective layer for LMBs due to its good  $\text{Li}^+$  conduction properties, high surface free energy, low  $\text{Li}^+$  diffusion barrier, wide electrochemical window and etc<sup>[13, 132-133]</sup>. Liu et al.<sup>[134]</sup> obtained excellent composites by coating and fluorinating LiF over 3D lithium/graphene (Li/G) surfaces. The 3D-structured LiF protective layer exhibits excellent electrochemical performance by improving Li utilization and inhibiting the accumulation of dead Li in the cell. The  $\text{LiC}_6$  formed in one of the 3D structures would maintain the entire framework and provide more electron paths, thus increasing the efficiency of the Li in the anode used to compensate for the Li loss during charging and discharging. The LiF protective layer on the 3D structure is more conducive to the homogeneous stripping and plating of Li substrates due to its high surface energy and low diffusion potential, while the protective layer also enhances the mechanical stability of the anode structure and prevents lithium metal from being eroded. Increasingly, carbon-based composite structures are being investigated as 3D collectors dedicated to the enhancement of LMA. Br is a strong lithium promoter with a high binding energy for lithium. Similarly, Br doping inhibits the formation of lithium dendrites and increases the cyclic stability of lithium metal. Duan's team<sup>[129]</sup> achieved homogeneous nucleation of Li in the conducting backbone by a two-step synergistic process through CuBr and Br doping modification of graphene-like films. CuBr reacts with Li metal forming LiBr, providing a

**Table 5 Performance of LMBs using composite with metal-carbide composites and fluoride/bromide/iodide as 3D current collectors**

Current collector	Half cell performance (Cycle number/h, CE)	Operating conditions (Current density/(mA cm <sup>-2</sup> ), Areal capacity/(mAh cm <sup>-2</sup> ))	Reference
Ti <sub>3</sub> C <sub>2</sub> Tx MXene films mixed with trace cellulose nanofibers	200, 98.9%	0.5, 2	[127]
AlF <sub>3</sub> particles embedded within carbon nanofibers	450, 97.2%	1, 1	[128]
CuBr- and Br-doped graphene-like film modified Cu foam	300, 98.8%	2, 2	[129]

fast Li diffusion channel to achieve uniform Li nucleation and inhibit dendrite growth (Fig. 7d). Due to the high binding energy of Br-doped sites and Li atoms, CuBr and Br-doped graphene-like thin films of modified copper foam (BGCF) are super lithophilic in order to strongly adsorb  $\text{Li}^+$  and further induce Li homogeneous nucleation.

## 8 Other carbon-based forms

In addition to the various methods mentioned above, other forms of carbon-based materials are also capable of stabilizing LMA. Graphdiyne (GDY) materials have  $\text{sp}^2$ -hybridized carbon atoms that are more lithophilic than other conventional carbon materials. Shang et al.<sup>[135]</sup> prepared ultrathin GDY nanofilms on Cu nanowires (CuNWs) *in situ* to form a 3D seamless coating with uniformly distributed lithophilic centers. CuNWs have a higher specific surface area than Cu, which provides more reaction sites. The introduction of GDY to form 3D self-supporting collectors not only provides many lithophilic centers, but also can accommodate lithium metal in large space. This achieves a nucleation overpotential smaller than the nucleation overpotential on the CuNW surface, which leads to the uniform accommodation of metallic Li in

the collector. As shown in Fig. 8a, the CuNW current collector produces non-uniformly growing lithium dendrites due to the inhomogeneous nucleation of lithium. In contrast to the CuNW current collector decorated with GDY, the lithium is uniformly distributed in the center of the lithophilicity, which suppresses dendrites and improves cycling performance. As shown in Fig. 8b, GDY@CuNW shows more stable performance at 350 h of cycling. This GDY@CuNW electrode is beneficial to the practical application of high energy density LMBs. Kang et al.<sup>[136]</sup> prepared nickel-anchored graphdiyne materials (Ni/GDY) on 3D copper foam by a solvothermal method. As shown in Fig. 8c, the synthesis of the GDY host is accomplished by a cross-coupling reaction for the precursor, followed by a two-step method for the deposition of nickel to obtain Ni/GDY from the synthetic GDY. GDY has a very high lithium storage capacity, while nickel is highly lithophilic. The rich nanoporous structure of GDY provides a stable lithium deposition interface for high efficiency and capacity of lithium deposition and stripping, and the introduction of the lithophilic group Ni-modified copper foam substrate can achieve a large area and a high rate of dendrite-free lithium deposition and stripping. The cyclic CE

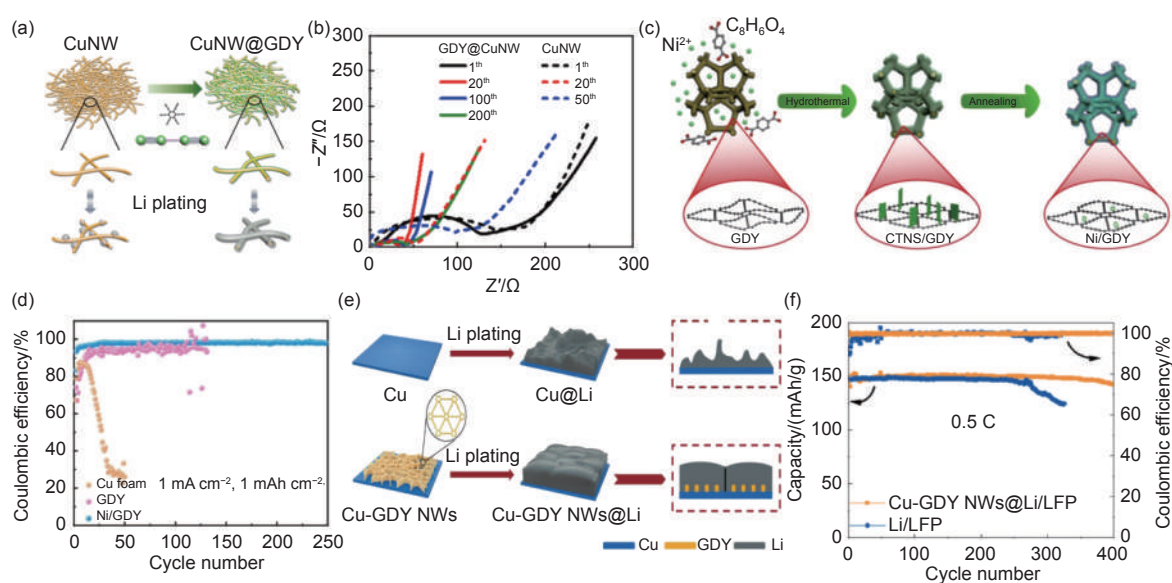


Fig. 8 (a) schematic process of the Li plating on bare CuNW and GDY@CuNW current collectors<sup>[135]</sup>. (b) impedance variations at different cycles (1.0 mA cm<sup>-2</sup>, 1.0 mAh cm<sup>-2</sup>)<sup>[135]</sup>. (c) Raman spectra of GDY and Ni/GDY<sup>[136]</sup>. (d) Under the conditions of 1 mA cm<sup>-2</sup>/1 mAh cm<sup>-2</sup>, the Li plating and stripping efficiency of Ni/GDY electrodes<sup>[136]</sup>. (e) Schematic lithium plating on bare Cu foil and Cu-GDY NWs<sup>[137]</sup>.

(f) Cycling performance of full cells with LFP at 0.5 C<sup>[137]</sup>. (Reprinted with permission)

of the lithium anode on three substrates of 1 mAh  $\text{cm}^{-2}$  is shown in Fig. 8d. The results showed that the CE of copper foam decreased sharply after 10 cycles, while the CE of GDY started to decrease after 120 cycles. Ni/GDY maintained 98.3% CE after 250 cycles and had good cycling performance. Zhu et al.<sup>[137]</sup> designed vertically aligned GDY nanowires (GDY NWs) uniformly grown on copper foils (Cu-GDY NWs) as 3D collectors to achieve stable dendrite-free LMA. The highly lithiophilic GDY NWs provide abundant and uniformly distributed active centers for lithium nucleation, resulting in unique columnar deposition of lithium without dendrites. As shown in Fig. 8e, the bare copper foil has a large raised surface, leading to uneven nucleation sites for Li deposition and causing uneven current density, resulting in the formation of a large number of Li dendrites. However, the highly lithiophilic GDY NWs on the copper foil provide abundant and uniformly distributed active sites for lithium nucleation and a uniformly distributed  $\text{Li}^+$  flux for lithium growth, leading to dendritic columnar deposition of lithium. In addition, Cu-GDY NWs@Li/LFP cells have excellent cycling stability. As shown in Fig. 8f, the capacity retention rate is 94.4% with 400 stable cycles at 0.5 C, while the Li/LFP cell decreases sharply after 253 cycles. At the same time, it is confirmed that the dendrite-free and stable LMA can be prepared by studying the GDY nanostructures with ideal structures. As shown in Table 6, the performance of some carbon-based materials compounded with other carbon-based forms as 3D collectors for LMBs is summarized.

## 9 Summary and outlook

LMBs have been under development for decades, but there is still a considerable amount of work to be done before they can be utilized commercially. In re-

cent decades, researchers have focused on developing more strategies to satisfy the requirements for security and stability and high energy storage in LMBs. In the last 20 years, advances in materials science and nanotechnology have made it possible to use carbon materials in a variety of battery systems. At the same time, anode materials have changed and new carbon-based materials have been made. Overall, carbon materials are used in LMBs in a variety of forms, each with its own unique advantages and disadvantages. Pure carbon materials have good stability and mechanical properties, but their lipophilic properties and storage capacity are limited. For pure carbon materials, the poor lithophilicity leads to inhomogeneous lithium deposition, bringing almost negligible dendrite suppression effect. However, due to the excellent electronic conductivity, mechanical strength and structural tunability of carbon, researchers have doped it with heteroatoms and compounded it with metal monomers/oxides/sulfides/selenides/phosphides/nitrides/carbides/iodides/fluorides with excellent lithium affinity to improve its affinity for lithium. When composited with these various metal compounds, due to the high reactivity of lithium, most of them would generate the corresponding metal monomers (or form alloys with lithium) and lithium compounds such as  $\text{Li}_2\text{O}$ ,  $\text{Li}_2\text{S}$ ,  $\text{Li}_2\text{Se}$ ,  $\text{Li}_x\text{P}$ ,  $\text{LiF}$  and etc. On the one hand, the generated Li-M alloy and lithium compounds, in addition to enhancing the interaction with ions, also modulate the components of the generated SEI and thus accelerate the diffusion of  $\text{Li}^+$ . On the other hand, these Li-M alloys involve an alloying de-alloying process of lithium, which obviously brings different volume expansion, and if the resulting SEI film cannot withstand this destructive process, it inevitably leads to unsatisfactory properties. The lithium com-

**Table 6 Performance of LMBs using composite with other carbon-based forms as 3D current collectors**

Current collector	Half cell performance (Cycle number/h, CE)	Operating conditions (Current density/(mA $\text{cm}^{-2}$ ), Areal capacity/(mAh $\text{cm}^{-2}$ ))	Reference
The CuNW electrode modified by GDY nanofilms	200, 96.5%	0.5, 0.5	[135]
Ni-anchored graphdiyne modified copper foam substrate	200, 98.5%	1, 1	[136]
grew GDY nanofilms on a Cu nanowire network	500, 99.2%	1, 2	[137]

pounds may precisely compensate for the weakness in this regard and could improve the mechanical strength and electron tunneling energy barriers of SEI, thus achieving different suppression of dendrites. As for the effect against dendrite inhibition, different Li-M alloys and Li<sub>2</sub>O and other lithium compounds involved in the SEI composition have different binding energy, ionic conductivity, and diffusion energy barriers for lithium, resulting in different dendrite inhibition effects. From the above analysis, metal/metal compound composite electrode with carbon-based materials has the boosted dendrite suppression effect, with some synergies, because there are always different permutations of lithium metal alloys and SEI inorganic components. However, it is always desired to obtain SEI with high electronic conductivity, negligible volume expansion during alloying-de-alloying, and high mechanical strength to enhance the diffusion of Li<sup>+</sup> while mitigating the concentration polarization or SEI is repeatedly destroyed and reconstructed, thus having the effect of suppressing dendrites. This paper deals with the application of carbon-based materials in LMBs. As shown in Fig. 9, when a battery is discharged, Li<sup>+</sup> move through the electrolyte to deposit the surface of the carbon-based scaffolds. The carbon-based scaffolds generally have high specific surface area and good electrical conductivity, which can homogenized Li<sup>+</sup> flux and provide electron transport

channels. However, due to the poor lithium affinity to Li<sup>+</sup>, the deposition of Li<sup>+</sup> on the surface of the pure carbonaceous scaffolds is not uniform, non-uniform deposition structures such as lithium dendrites and lithium needles are easily formed. These uneven deposition structures can cause uneven pressure inside the battery and generate internal stress, which can easily cause safety problems such as short circuit and leakage, and affect the performance and life of the battery. To solve this problem, lithiophilic heteroatoms, functional groups, elemental metal/metal oxide/sulfide/selenide/nitride/phosphide/carbide/iodide/fluoride, are introduced to carbon scaffolds to increase affinity for lithium, in addition of the synergy effects of porous structure and good conductivity, not only the Li<sup>+</sup> flow is homogenized but also the transmission rates of Li<sup>+</sup> are enhanced, result in the reduced concentration difference polarization thus the growth of dendrite is inhibited and homogeneous deposition of Li<sup>+</sup> is achieved and improved battery cycle life and safety performance.

Porous carbonaceous collectors provide high specific surface area, variable electronic conductivity, light weight, chemical stability and high mechanical strength, which efficiently lower the current density, raise the energy density, and suppress dendrite formation, thus provide enough storage area and safety ability for active lithium. The incorporation of het-

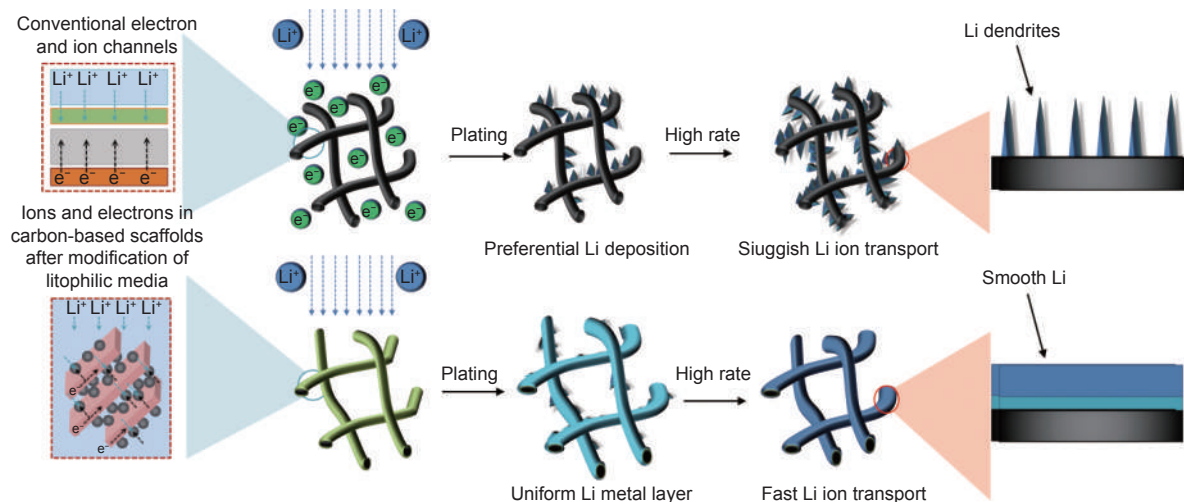


Fig. 9 Mechanism of carbonaceous scaffolds in LMBs

eroatoms or functional groups with lithiophilic characteristics (N, S and P, et al.) into porous carbon as a 3D collector to stabilize the lithium metal approach minimizes the nucleation overpotential of  $\text{Li}^+$  on the lithium metal surface and enhances lithium inhomogeneous deposition. Similarly, it has also been shown that heteroatoms or functional groups modified carbon-based materials with metal monomers also can significantly improve the lithiophilic behaviors, generally provides nucleation sites and enhance ion diffusion. As a 3D current collector, the carbon-based materials have functional groups on its surface that can mix with metal oxides, metal nitrides and metal carbides. In LMBs, metal ions are extremely lithophilicity and conductors. Combining with carbon-based materials, Li metal could greatly enhance the overall electronic conductivity of metal cells, enhance electron/ion transport, and limit lithium dendrite development. It is foreseeable that carbon materials would continue to be an important part for energy storage and they would also keep the flame of development going. Despite of the carbon-based materials have made great achievements in LMA, for the practical application of LMBs, there are still some practical operating conditions issues need to be further explored and discussed.

(1) Although carbon-based materials as 3D current collectors will obtain a large specific surface area, which can effectively inhibit the growth of lithium dendrites and reduce the current density, it will also make the contact area between lithium and the electrolyte larger, resulting in many side reactions that are not conducive to development and reducing the utilization rate of lithium.

(2) Lithium will inevitably react with a part of carbon, resulting in the instability of the carbon structure and a decrease in its mechanical strength, so that the LMA material becomes fragile and reduces the safety and stability of the battery.

(3) At present, the mechanism of lithium metal growth of Li dendrites has not been completely explained. In order to better design a more researchable high-performance carbon-based LMA, we need to

continue to conduct theoretical research on the formation mechanism of Li dendrites.

(4) To improve the energy density of LMBs and improve electrochemical activity, we need to study the anode material with a carbon-based multi-dimensional or composite structure and make a reasonable design of the surface chemistry of the carbon material as needed.

(5) At present, there are differences in electrochemical test conditions, which is not conducive to the comparison of modifications of different carbon-based materials. We therefore need to unify the test standards for LMA to develop more efficient carbon-based anode materials.

(6) On the basis of structural regulation, it is necessary to continuously develop the electrolyte and regulate the electrode interface. Find electrolytes that work well with high-voltage cathode materials and are good for commercial development, and keep improving the electrode interface to increase the CE and cycle stability.

(7) To get carbon-based materials into commercial LMBs, we need to keep researching and making carbon-based materials that are simple and easy to scale up, and keep improving the manufacturing technologies.

## Acknowledgements

This work was supported by the National Natural Science Foundation of China (52272194), Liaoning Revitalization Talents Program (XLYC2007155), the Fundamental Research Funds for the Central Universities (N2025018, N2025009). This manuscript was written through the contributions of all the authors. All authors have given approval to the final version of the manuscript.

## References

- [1] Gür T M. Review of electrical energy storage technologies, materials and systems: challenges and prospects for large-scale grid storage[J]. *Energy & Environmental Science*, 2018, 11(10): 2696-2767 DOI: 10.1039/C8EE01419A .
- [2] Carley S, Konisky D M. The justice and equity implications of the

- clean energy transition[J]. *Nature Energy*, 2020, 5(8): 569-577.
- [ 3 ] Friedlingstein P, O'Sullivan M, Jones M W, et al. Global carbon budget 2020[J]. *Earth System Science Data*, 2020, 12(4): 3269-3340.
- [ 4 ] Zhao X, Ma X, Chen B, et al. Challenges toward carbon neutrality in China: Strategies and countermeasures [J]. *Resources Conservation And Recycling*, 2022, 176:105959 DOI:10.1016/j.resconrec.2021.105959.
- [ 5 ] Fleischmann S, Mitchell J B, Wang R, et al. Pseudocapacitance: From fundamental understanding to high power energy storage materials[J]. *Chemical Reviews*, 2020, 120(14): 6738-6782.
- [ 6 ] Koochi-Fayegh S, Rosen M A. A review of energy storage types, applications and recent developments[J]. *Journal of Energy Storage*, 2020, 27: 101047.
- [ 7 ] Reddy M V, Mauger A, Julien C M, et al. Brief history of early lithium-battery development [J]. *Materials*, 2020, 13(8):1884 DOI:10.3390/ma13081884.
- [ 8 ] Cheng X B, Zhang R, Zhao C Z, et al. Toward safe lithium metal anode in rechargeable batteries: A review[J]. *Chemical Reviews*, 2017, 117(15): 10403-10473.
- [ 9 ] Wang J B, Ren Z, Hou Y, et al. A review of graphene synthesis at low temperatures by CVD methods[J]. *New Carbon Materials*, 2020, 35(3): 193-208.
- [ 10 ] Jin L, Zhang H, Li S, et al. Exchange of Li and AgNO<sub>3</sub> enabling stable 3D lithium metal anodes with embedded lithophilic nanoparticles and a solid electrolyte interphase inducer[J]. *Acs Applied Materials & Interfaces*, 2021, 13(32): 38425-38431 DOI:10.1021/acsami.1c11733 .
- [ 11 ] Fan E, Li L, Wang Z, et al. Sustainable recycling technology for Li-ion batteries and beyond: Challenges and future prospects[J]. *Chemical Reviews*, 2020, 120(14): 7020-7063.
- [ 12 ] Wu F, Maier J, Yu Y. Guidelines and trends for next-generation rechargeable lithium and lithium-ion batteries[J]. *Chemical Society Reviews*, 2020, 49(5): 1569-1614.
- [ 13 ] Zhang Y, Zuo T T, Popovic J, et al. Towards better Li metal anodes: Challenges and strategies[J]. *Materials Today*, 2020, 33: 56-74.
- [ 14 ] Liang Y, Xiao Y, Yan C, et al. A bifunctional ethylene-vinyl acetate copolymer protective layer for dendrites-free lithium metal anodes[J]. *Journal of Energy Chemistry*, 2020, 48: 203-207.
- [ 15 ] Zhang C, Huang Z, Lv W, et al. Carbon enables the practical use of lithium metal in a battery[J]. *Carbon*, 2017, 123: 744-755.
- [ 16 ] Chen T, Wu H P, Wan J, et al. Synthetic poly-dioxolane as universal solid electrolyte interphase for stable lithium metal anodes[J]. *Journal of Energy Chemistry*, 2021, 62: 172-178.
- [ 17 ] Wang Z, Qi F, Yin L, et al. An anion-tuned solid electrolyte interphase with fast ion transfer kinetics for stable lithium anodes [J]. *Advanced Energy Materials*, 2020, 10(14):1903843 DOI:10.1002/aenm.201903843.
- [ 18 ] Qian H, Li X. Progress in functional solid electrolyte interphases for boosting Li metal anode [J]. *Acta Physico-Chimica Sinica*, 2021, 37(2).
- [ 19 ] Zhang X L, Ruan Z Q, He Q T, et al. Three-dimensional (3D) nanostructured skeleton substrate composed of hollow carbon fiber/carbon nanosheet/ZnO for stable lithium anode[J]. *ACS Applied Materials & Interfaces*, 2021, 13(2): 3078-3088.
- [ 20 ] Wu H, Jia H, Wang C, et al. Recent progress in understanding solid electrolyte interphase on lithium metal anodes[J]. *Advanced Energy Materials*, 2021, 11(5): 1-15.
- [ 21 ] Zhai P, Wang T, Jiang H, et al. 3D artificial solid-electrolyte interphase for lithium metal anodes enabled by insulator-metal-insulator layered heterostructures[J]. *Advanced Materials*, 2021, 33(13): 2006247.
- [ 22 ] Lu Q, Jie Y, Meng X, et al. Carbon materials for stable Li metal anodes: Challenges, solutions, and outlook[J]. *Carbon Energy*, 2021, 3(6): 957-975.
- [ 23 ] Meda U S, Lal L, Sushantha M, et al. Solid electrolyte interphase (SEI), a boon or a bane for lithium batteries: A review on the recent advances [J]. *Journal of Energy Storage*, 2021: 103564 DOI:10.1016/j.est.2021.103564.
- [ 24 ] Shan X, Zhong Y, Zhang L, et al. A brief review on solid electrolyte interphase composition characterization technology for lithium metal batteries: Challenges and perspectives[J]. *Journal Of Physical Chemistry C*, 2021, 125(35): 19060-19080.
- [ 25 ] Yan T, Li F, Xu C, et al. Highly uniform lithiated Nafion thin coating on separator as an artificial SEI layer of lithium metal anode toward suppressed dendrite growth[J]. *Electrochimica Acta*, 2022, 410: 140004.
- [ 26 ] Jumi K I M, Jimin O, Kim J Y, et al. Recent progress and perspectives of solid electrolytes for lithium rechargeable batteries[J]. *Journal of the Korean Electrochemical Society*, 2019, 22(3): 87-103.
- [ 27 ] Nie K, Hong Y, Qiu J, et al. Interfaces between cathode and electrolyte in solid state lithium batteries: Challenges and perspectives[J]. *Frontiers In Chemistry*, 2018, 6: 616.
- [ 28 ] Zhao C Z, Duan H, Huang J Q, et al. Designing solid-state interfaces on lithium-metal anodes: a review[J]. *Science China-Chemistry*, 2019, 62(10): 1286-1299.
- [ 29 ] Kang D, Xiao M, Lemmon J P. Artificial solid-electrolyte interphase for lithium metal batteries[J]. *Batteries & Supercaps*, 2021, 4(3): 445-455.
- [ 30 ] Jin C B, Shi P, Zhang X Q, et al. Advances in carbon materials for stable lithium metal batteries[J]. *New Carbon Materials*, 2022, 37(1): 1-24.
- [ 31 ] Liu Y, Zhai Y, Xia Y, et al. Recent progress of porous materials in lithium-metal batteries[J]. *Small Structures*, 2021, 2(5):

- 2000118.
- [ 32 ] Chen L, Ding K, Li K, et al. Crystalline porous materials-based solid-state electrolytes for lithium metal batteries[J]. *Energy Chem*, 2022, 4(3): 100073.
- [ 33 ] Li N, Wei W, Xie K, et al. Suppressing dendritic lithium formation using porous media in lithium metal-based batteries[J]. *Nano Letters*, 2018, 18(3): 2067-2073.
- [ 34 ] Jin C, Sheng O, Luo J, et al. 3D lithium metal embedded within lithiophilic porous matrix for stable lithium metal batteries[J]. *Nano Energy*, 2017, 37: 177-186.
- [ 35 ] Yun Q, He Y B, Lv W, et al. Chemical dealloying derived 3D porous current collector for li metal anodes[J]. *Advanced Materials*, 2016, 28(32): 6932-+.
- [ 36 ] Guo C, Zhang W, Tu J, et al. Construction of 3D copper-based collector and its application in lithium metal batteries[J]. *Progress In Chemistry*, 2022, 34(2): 370-383.
- [ 37 ] Chen J Y, Zhao J, Lei L N, et al. Dynamic intelligent Cu current collectors for ultrastable lithium metal anodes[J]. *Nano Letters*, 2020, 20(5): 3403-3410.
- [ 38 ] Zhang D, Dai A, Wu M, et al. Lithiophilic 3D porous cuzn current collector for stable lithium metal batteries[J]. *ACS Energy Letters*, 2020, 5(1): 180-186.
- [ 39 ] Lu Z, Liang Q, Wang B, et al. Graphitic carbon nitride induced micro-electric field for dendrite-free lithium metal anodes[J]. *Advanced Energy Materials*, 2019, 9(7): 1803186.
- [ 40 ] Pu J, Li J, Zhang K, et al. Conductivity and lithiophilicity gradients guide lithium deposition to mitigate short circuits[J]. *Nature Communications*, 2019, 10(1): 1-10.
- [ 41 ] Shang J, Yu W, Wang L, et al. Metallic glass-fiber fabrics: a new type of flexible, super-lightweight, and 3D current collector for lithium batteries[J]. *Advanced Materials*, 2023, 35: 2211748.
- [ 42 ] Jin S, Jiang Y, Ji H, et al. Advanced 3D current collectors for lithium-based batteries[J]. *Advanced Materials*, 2018, 30(48): 1802014.
- [ 43 ] Xia Y, Hu W, Yao Y, et al. Application of electrodeposited Cu-metal nanoflake structures as 3D current collector in lithium-metal batteries[J]. *Nanotechnology*, 2022, 33(24): 1361-6528.
- [ 44 ] Zhang L, Jin Q, Zhao K, et al. 3D hierarchical Cu@Ag nanostructure as a current collector for dendrite-free lithium metal anode[J]. *Dalton Transactions*, 2022, 51(43): 16565-16573.
- [ 45 ] Yang S, Cheng Y, Xiao X, et al. Development and application of carbon fiber in batteries[J]. *Chemical Engineering Journal*, 2020, 384: 123294.
- [ 46 ] Tang K, Xiao J, Li X, et al. Advances of carbon-based materials for lithium metal anodes[J]. *Frontiers In Chemistry*, 2020, 8: 595972.
- [ 47 ] Fu A, Wang C, Pei F, et al. Recent advances in hollow porous carbon materials for lithium-sulfur batteries[J]. *Small*, 2019, 15(10): 1804786.
- [ 48 ] Wu Z, Sun K, Wang Z. A review of the application of carbon materials for lithium metal batteries[J]. *Batteries-Basel*, 2022, 8(11): 246.
- [ 49 ] Deng W, Zhu W, Zhou X, et al. Graphene nested porous carbon current collector for lithium metal anode with ultrahigh areal capacity[J]. *Energy Storage Materials*, 2018, 15: 266-273.
- [ 50 ] Chen H, Yang Y, Boyle D T, et al. Free-standing ultrathin lithium metal-graphene oxide host foils with controllable thickness for lithium batteries[J]. *Nature Energy*, 2021, 6(8): 790-798.
- [ 51 ] Sun C, Liu Y, Sheng J, et al. Status and prospects of porous graphene networks for lithium-sulfur batteries[J]. *Materials Horizons*, 2020, 7(10): 2487-2518.
- [ 52 ] Xu Q, Yang X, Rao M, et al. High energy density lithium metal batteries enabled by a porous graphene/MgF<sub>2</sub> framework[J]. *Energy Storage Materials*, 2020, 26: 73-82.
- [ 53 ] Lu K, Xu H, He H, et al. Modulating reactivity and stability of metallic lithium via atomic doping[J]. *Journal of Materials Chemistry A*, 2020, 8(20): 10363-10369.
- [ 54 ] Chen X, Chen X R, Hou T Z, et al. Lithiophilicity chemistry of heteroatom-doped carbon to guide uniform lithium nucleation in lithium metal anodes[J]. *Science Advances*, 2019, 5(2): eaau7728.
- [ 55 ] Yuan Y, Chen Z, Yu H, et al. Heteroatom-doped carbon-based materials for lithium and sodium ion batteries[J]. *Energy Storage Materials*, 2020, 32: 65-90.
- [ 56 ] Wu Y, Rahm E, Holze R. Effects of heteroatoms on electrochemical performance of electrode materials for lithium ion batteries[J]. *Electrochimica Acta*, 2002, 47(21): 3491-3507.
- [ 57 ] Shao R, Zhu F, Cao Z, et al. Heteroatom-doped carbon networks enabling robust and flexible silicon anodes for high energy Li-ion batteries[J]. *Journal of Materials Chemistry A*, 2020, 8(35): 18338-18347.
- [ 58 ] Pappas G S, Ferrari S, Huang X, et al. Heteroatom doped-carbon nanospheres as anodes in lithium ion batteries[J]. *Materials*, 2016, 9(1): 35.
- [ 59 ] Wang Y, Yuan C, Li K, et al. Freestanding porous silicon@ heteroatom-doped porous carbon fiber anodes for high-performance lithium-ion batteries[J]. *ACS Applied Energy Materials*, 2022, 5(9): 11462-11471.
- [ 60 ] Dai C, Sun G, Hu L, et al. Recent progress in graphene-based electrodes for flexible batteries[J]. *Infomat*, 2020, 2(3): 509-526.
- [ 61 ] Xu Z, Zhang P, Chen J, et al. Growth and growth mechanism of oxide nanocrystals on electrochemically exfoliated graphene for lithium storage[J]. *Energy Storage Materials*, 2019, 18: 174-181.
- [ 62 ] Seyyedini S T, Yafthian M R, Sovizi M R. Cobalt oxyhydroxide/graphene oxide nanocomposite for amelioration of electrochemical performance of lithium/sulfur batteries[J].

- Journal of Solid State Electrochemistry, 2017, 21(3): 649-656.
- [ 63 ] Zhang L, Ma T, Yang Y W, et al. Pomegranate-inspired graphene parcel enables high-performance dendrite-free lithium metal anodes[J]. *Advanced Science*, 2022, 9(28): 2203178.
- [ 64 ] Zhang M, Shan Y, Kong Q, et al. Applications of metal-organic framework-graphene composite materials in electrochemical energy storage[J]. *Flatchem*, 2022, 32: 100332.
- [ 65 ] Yang Y, Ai L, Yu S, et al. 3D-printed porous go framework enabling dendrite-free lithium-metal anodes[J]. *ACS Applied Energy Materials*, 2022, 5(12): 15666-15672.
- [ 66 ] Li N, Gan F, Wang P, et al. In situ synthesis of 3D sulfur-doped graphene/sulfur as a cathode material for lithium-sulfur batteries[J]. *Journal of Alloys and Compounds*, 2018, 754: 64-71.
- [ 67 ] Zhu J, Tu W, Pan H, et al. Self-templating synthesis of hollow  $\text{Co}_3\text{O}_4$  nanoparticles embedded in N, S-dual-doped reduced graphene oxide for lithium ion batteries[J]. *ACS Nano*, 2020, 14(5): 5780-5787.
- [ 68 ] Zhang F, Liu X, Yang M, et al. Novel S-doped ordered mesoporous carbon nanospheres toward advanced lithium metal anodes[J]. *Nano Energy*, 2020, 69: 104443.
- [ 69 ] Choi Y J, Lee G W, Kim Y H, et al. Microspherical assembly of selectively pyridinic N-doped nanoporated graphene for stable Li-metal anodes: Synergistic coupling of lithiophilic pyridinic N on perforation edges and low tortuosity via graphene nanoporation[J]. *Chemical Engineering Journal*, 2023, 455: 140770.
- [ 70 ] Fang Y, Hsieh Y Y, Khosravifar M, et al. Lithiophilic current collector based on nitrogen doped carbon nanotubes and three-dimensional graphene for long-life lithium metal batteries[J]. *Materials Science and Engineering:B*, 2021, 267: 115067.
- [ 71 ] Huang G, Han J, Zhang F, et al. Lithiophilic 3D nanoporous nitrogen-doped graphene for dendrite-free and ultrahigh-rate lithium-metal anodes[J]. *Advanced Materials*, 2019, 31(2): 1805334.
- [ 72 ] Zhang R, Wen S, Wang N, et al. N-doped graphene modified 3D porous Cu current collector toward microscale homogeneous Li deposition for Li metal anodes[J]. *Advanced Energy Materials*, 2018, 8(23): 1800914.
- [ 73 ] Qiao L, Zhang R, Li Y, et al. Super-assembled hierarchical and stable N-doped carbon nanotube nanoarrays for dendrite-free lithium metal batteries[J]. *ACS Applied Energy Materials*, 2021, 5(1): 815-824.
- [ 74 ] Wang H, An D, Tian P, et al. Incorporating quantum-sized boron dots into 3D cross-linked rGO skeleton to enable the activity of boron anode for favorable lithium storage[J]. *Chemical Engineering Journal*, 2021, 425: 130659.
- [ 75 ] An Y, Tian Y, Li Y, et al. Heteroatom-doped 3D porous carbon architectures for highly stable aqueous zinc metal batteries and non-aqueous lithium metal batteries[J]. *Chemical Engineering Journal*, 2020, 400: 125843.
- [ 76 ] Lu C, Tian M, Wei C, et al. Synergized N, P dual-doped 3D carbon host derived from filter paper for durable lithium metal anodes[J]. *Journal of Colloid and Interface Science*, 2023, 632: 1-10.
- [ 77 ] Li H, Liu J, Zhang Y, et al. Mono-atom dispersed graphene foam with nitrogen-doped carbon nanospheres used in preparation of anode material for lithium-sulfur battery, is grown with carbon nanospheres doped with nitrogen atoms and single metal atoms, CN113104840-A [P/OL].
- [ 78 ] Wang J, Han W Q. A review of heteroatom doped materials for advanced lithium-sulfur batteries[J]. *Advanced Functional Materials*, 2022, 32(2): 07166.
- [ 79 ] Wu J, Pan Z, Zhang Y, et al. The recent progress of nitrogen-doped carbon nanomaterials for electrochemical batteries[J]. *Journal of Materials Chemistry A*, 2018, 6(27): 12932-12944.
- [ 80 ] Gao C, Li J, Sun K, et al. Controllable lithium deposition behavior hollow of N, O co-doped carbon nanospheres for practical lithium metal batteries[J]. *Chemical Engineering Journal*, 2021, 412: 128721.
- [ 81 ] Tang K, Xiao J, Long M, et al. Superlithiophilic N, S-codoped carbon on Ni foam as a stable 3D host for dendrite-free Li metal anodes[J]. *Sustainable Materials and Technologies*, 2022, 32: e00408.
- [ 82 ] Chen T, Jia W, Yao Z, et al. Partly lithiated graphitic carbon foam as 3D porous current collectors for dendrite-free lithium metal anodes[J]. *Electrochemistry Communications*, 2019, 107: 106535.
- [ 83 ] Kwon H, Lee J H, Roh Y, et al. An electron-deficient carbon current collector for anode-free Li-metal batteries[J]. *Nature Communications*, 2021, 12(1): 5537.
- [ 84 ] Yang G, Li Y, Tong Y, et al. Lithium plating and stripping on carbon nanotube sponge[J]. *Nano Letters*, 2019, 19(1): 494-499.
- [ 85 ] Huang Z, Kong D, Zhang Y, et al. Vertical graphenes grown on a flexible graphite paper as an all-carbon current collector towards stable li deposition [J]. *Research*, 2020:7163948 DOI: 10.34133/2020/7163948.
- [ 86 ] Meng Q, Deng B, Zhang H, et al. Heterogeneous nucleation and growth of electrodeposited lithium metal on the basal plane of single-layer graphene[J]. *Energy Storage Materials*, 2019, 16: 419-425.
- [ 87 ] Zhai P, Wang T, Yang W, et al. Uniform lithium deposition assisted by single-atom doping toward high-performance lithium metal anodes [J]. *Advanced Energy Materials*, 2019, 9(18):1804019 DOI:10.1002/aenm.201804019.
- [ 88 ] Ye H, Xin S, Yin Y X, et al. Stable li plating/stripping electrochemistry realized by a hybrid li reservoir in spherical

- carbon granules with 3D conducting skeletons[J]. *Journal of the American Chemical Society*, 2017, 139(16): 5916-5922.
- [ 89 ] Sun Y, Zhao W, Wang X, et al. Progress of carbon and metal-based three-dimensional materials for dendrite-proof and interface-compatible lithium metal anode[J]. *Applied Surface Science*, 2022, 598: 153785.
- [ 90 ] Tian B, Huang Z, Xu X, et al. Three-dimensional Ag/carbon nanotube-graphene foam for high performance dendrite free lithium/sodium metal anodes[J]. *Journal of Materials Science & Technology*, 2023, 132: 50-58.
- [ 91 ] Yang C, Yao Y, He S, et al. Ultrafine silver nanoparticles for seeded lithium deposition toward stable lithium metal anode[J]. *Advanced Materials*, 2017, 29(38): 1702714.
- [ 92 ] Sun Q, Zhai W, Hou G, et al. In situ synthesis of a lithiophilic ag-nanoparticles-decorated 3D porous carbon framework toward dendrite-free lithium metal anodes[J]. *ACS Sustainable Chemistry & Engineering*, 2018, 6(11): 15219-15227.
- [ 93 ] Hou G, Ren X, Ma X, et al. Dendrite-free Li metal anode enabled by a 3D free-standing lithiophilic nitrogen-enriched carbon sponge[J]. *Journal of Power Sources*, 2018, 386: 77-84.
- [ 94 ] Xue P, Liu S, Shi X, et al. A hierarchical silver-nanowire-graphene host enabling ultrahigh rates and superior long-term cycling of lithium-metal composite anodes[J]. *Advanced Materials*, 2018, 30(44): 1804165.
- [ 95 ] Yan K, Lu Z, Lee H W, et al. Selective deposition and stable encapsulation of lithium through heterogeneous seeded growth[J]. *Nature Energy*, 2016, 1(3): 16010.
- [ 96 ] Lan X, Ye W, Zheng H, et al. Encapsulating lithium and sodium inside amorphous carbon nanotubes through gold-seeded growth[J]. *Nano Energy*, 2019, 66: 104178.
- [ 97 ] Li D, Gao Y, Xie C, et al. Au-coated carbon fabric as Janus current collector for dendrite-free flexible lithium metal anode and battery[J]. *Applied Physics Reviews*, 2022, 9(1): 011424.
- [ 98 ] Xu K, Zhu M, Wu X, et al. Dendrite-tamed deposition kinetics using single-atom Zn sites for Li metal anode[J]. *Energy Storage Materials*, 2019, 23: 587-593.
- [ 99 ] Matsui M. Study on electrochemically deposited Mg metal[J]. *Journal of Power Sources*, 2011, 196(16): 7048-7055.
- [ 100 ] Ling C, Banerjee D, Matsui M. Study of the electrochemical deposition of Mg in the atomic level: Why it prefers the non-dendritic morphology[J]. *Electrochimica Acta*, 2012, 76: 270-274.
- [ 101 ] Ding Y, Hu L, He D, et al. Design of multishell microsphere of transition metal oxides/carbon composites for lithium ion battery[J]. *Chemical Engineering Journal*, 2020, 380: 122489.
- [ 102 ] Tan X, Wu Y, Lin X, et al. Application of MOF-derived transition metal oxides and composites as anodes for lithium-ion batteries[J]. *Inorganic Chemistry Frontiers*, 2020, 7(24): 4939-4955.
- [ 103 ] Reddy R C K, Lin J, Chen Y, et al. Progress of nanostructured metal oxides derived from metal-organic frameworks as anode materials for lithium-ion batteries[J]. *Coordination Chemistry Reviews*, 2020, 420: 213434.
- [ 104 ] Yu B, Tao T, Mateti S, et al. Nanoflake arrays of lithiophilic metal oxides for the ultra-stable anodes of lithium-metal batteries[J]. *Advanced Functional Materials*, 2018, 28(36): 1803023.
- [ 105 ] Yu Z, Qu X, Dou A, et al. Carbon-coated cation-disordered rocksalt-type transition metal oxide composites for high energy Li-ion batteries[J]. *Ceramics International*, 2021, 47(2): 1758-1765.
- [ 106 ] Xiang M, Wu H, Liu H, et al. A flexible 3D multifunctional MgO-decorated carbon foam@ CNTs hybrid as self-supported cathode for high-performance lithium-sulfur batteries[J]. *Advanced Functional Materials*, 2017, 27(37): 1702573.
- [ 107 ] Zhang Y, Liu B, Hitz E, et al. A carbon-based 3D current collector with surface protection for Li metal anode[J]. *Nano Research*, 2017, 10(4): 1356-1365.
- [ 108 ] Wang T S, Liu X, Wang Y, et al. High areal capacity dendrite-free li anode enabled by metal-organic framework-derived nanorod array modified carbon cloth for solid state li metal batteries[J]. *Advanced Functional Materials*, 2021, 31(2): 2001973.
- [ 109 ] Yue X Y, Bao J, Qiu Q Q, et al. Copper decorated ultralight 3D carbon skeleton derived from soybean oil for dendrite-free Li metal anode[J]. *Chemical Engineering Journal*, 2020, 391: 123516.
- [ 110 ] Zeng L, Zhou T, Xu X, et al. General construction of lithiophilic 3D skeleton for dendrite-free lithium metal anode via a versatile MOF-derived route[J]. *Science China-Materials*, 2022, 65(2): 337-348.
- [ 111 ] Xu C, Wang H, Liu X, et al. Lithiophilic vanadium oxide coated three-dimensional carbon network design towards stable lithium metal anode[J]. *Journal of Power Sources*, 2023, 562: 232778.
- [ 112 ] Ye C, Zhang L, Guo C, et al. A 3D hybrid of chemically coupled nickel sulfide and hollow carbon spheres for high performance lithium-sulfur batteries[J]. *Advanced Functional Materials*, 2017, 27(33): 1702524.
- [ 113 ] He J, Manthiram A. 3D CoSe@ C aerogel as a host for dendrite-free lithium-metal anode and efficient sulfur cathode in Li-S full cells[J]. *Advanced Energy Materials*, 2020, 10(41): 2002654.
- [ 114 ] Gao C, Hong B, Sun K, et al. Self-suppression of lithium dendrite with aluminum nitride nanoflake additive in 3D carbon paper for lithium metal batteries[J]. *Energy Technology*, 2020, 8(7): 1901463.
- [ 115 ] Zhu J, Chen J, Luo Y, et al. Lithiophilic metallic nitrides modified nickel foam by plasma for stable lithium metal anode[J]. *Energy Storage Materials*, 2019, 23: 539-546.
- [ 116 ] Song Z, Liu Y, Wang Z, et al. Synergistic modulation of Li

- nucleation/growth enabled by CNTs-wrapped lithiophilic CoP/Co<sub>2</sub>P decorated hollow carbon polyhedron host for stable lithium metal anodes [J]. *Nano Research*, 2023;4961–4969 DOI: 10.1007/s12274-022-5179-4.
- [ 117 ] Cao W, Chen W, Lu M, et al. In situ generation of Li<sub>3</sub>N concentration gradient in 3D carbon-based lithium anodes towards highly-stable lithium metal batteries[J]. *Journal of Energy Chemistry*, 2023, 76: 648-656.
- [ 118 ] Luo L, Li J, Yaghoobnejad Asl H, et al. A 3D lithiophilic Mo<sub>2</sub>N-modified carbon nanofiber architecture for dendrite-free lithium-metal anodes in a full cell[J]. *Advanced Materials*, 2019, 31(48): 1904537.
- [ 119 ] Wang Z, Wang J, Mao Q, et al. Uniform lithium deposition and dissolution via metallic phosphides medium for stable cycling lithium metal batteries[J]. *Chemical Engineering Journal*, 2021, 407: 126861.
- [ 120 ] Zhang X, Jin S, Seo M H, et al. Hierarchical porous structure construction for highly stable self-supporting lithium metal anode[J]. *Nano Energy*, 2022, 93: 106905.
- [ 121 ] Zhang W, Jin H, Du Y, et al. Sulfur and nitrogen codoped Nb<sub>2</sub>C MXene for dendrite-free lithium metal battery[J]. *Electrochimica Acta*, 2021, 390: 138812.
- [ 122 ] Shi H, Yue M, Zhang C J, et al. 3D flexible, conductive, and recyclable Ti<sub>3</sub>C<sub>2</sub>T<sub>x</sub> mxene-melamine foam for high-areal-capacity and long-lifetime alkali-metal anode[J]. *ACS Nano*, 2020, 14(7): 8678-8688.
- [ 123 ] Tian Y, An Y, Wei C, et al. Flexible and free-standing Ti<sub>3</sub>C<sub>2</sub>T<sub>x</sub> mxene@zn paper for dendrite-free aqueous zinc metal batteries and nonaqueous lithium metal batteries[J]. *ACS Nano*, 2019, 13(10): 11676-11685.
- [ 124 ] Chen Q, Wei Y, Zhang X, et al. Vertically aligned mxene nanosheet arrays for high-rate lithium metal anodes[J]. *Advanced Energy Materials*, 2022, 12(18): 2200072.
- [ 125 ] Shen Y, Pu Z, Zhang Y, et al. MXene/ZnO flexible freestanding film as a dendrite-free support in lithium metal batteries[J]. *Journal of Materials Chemistry A*, 2022, 10(33): 17199-17207.
- [ 126 ] Fang Y Z, Liang S, Zhang X, et al. Li (110) lattice plane evolution induced by a 3D MXene skeleton for stable lithium metal anodes[J]. *Chemical Communications*, 2022, 58(67): 9373-9376.
- [ 127 ] Wang C Y, Zheng Z J, Feng Y Q, et al. Topological design of ultrastrong MXene paper hosted Li enables ultrathin and fully flexible lithium metal batteries[J]. *Nano Energy*, 2020, 74: 104817.
- [ 128 ] Guo C, Yang H, Naveed A, et al. AlF<sub>3</sub>-Modified carbon nanofibers as a multifunctional 3D interlayer for stable lithium metal anodes[J]. *Chemical Communications*, 2018, 54(60): 8347-8350.
- [ 129 ] Duan H, Zhang J, Chen X, et al. Uniform nucleation of lithium in 3D current collectors via bromide intermediates for stable cycling lithium metal batteries[J]. *Journal of the American Chemical Society*, 2018, 140(51): 18051-18057.
- [ 130 ] Shi H, Zhang C J, Lu P, et al. Conducting and lithiophilic mxene/graphene framework for high-capacity, dendrite-free lithium-metal anodes[J]. *ACS Nano*, 2019, 13(12): 14308-14318.
- [ 131 ] Xia Y, Mathis T S, Zhao M Q, et al. Thickness-independent capacitance of vertically aligned liquid-crystalline MXenes[J]. *Nature*, 2018, 557(7705): 409-412.
- [ 132 ] Tan J, Matz J, Dong P, et al. A growing appreciation for the role of lif in the solid electrolyte interphase[J]. *Advanced Energy Materials*, 2021, 11(16): 2100046.
- [ 133 ] Zhao J, Liao L, Shi F, et al. Surface fluorination of reactive battery anode materials for enhanced stability[J]. *Journal of the American Chemical Society*, 2017, 139(33): 11550-11558.
- [ 134 ] Liu Z, He B, Zhang Z, et al. Lithium/graphene composite anode with 3D structural lif protection layer for high-performance lithium metal batteries[J]. *ACS Applied Materials & Interfaces*, 2022, 14(2): 2871-2880.
- [ 135 ] Shang H, Zuo Z, Li Y. Highly lithiophilic graphdiyne nanofilm on 3D free-standing Cu nanowires for high-energy-density electrodes[J]. *ACS Applied Materials & Interfaces*, 2019, 11(19): 17678-17685.
- [ 136 ] Kang H, Hua B, Gao P, et al. Ni/Graphdiyne composites inhibit dendrite growth in lithium metal anodes[J]. *Electrochimica Acta*, 2023, 440: 141744.
- [ 137 ] Zhu M, Yin C, Wang Q, et al. Columnar lithium deposition guided by graphdiyne nanowalls toward a stable lithium metal anode[J]. *ACS Applied Materials & Interfaces*, 2022, 14(50): 55700-55708.

